Neurobiology of Disease 129 (2019) 79–92

Contents lists available at ScienceDirect

Neurobiology of Disease

journal homepage: www.elsevier.com/locate/ynbdi

In-vivo genetic ablation of metabotropic glutamate receptor type 5 slows down disease progression in the SOD1^{G93A} mouse model of amyotrophic lateral sclerosis

Tiziana Bonifacino[a], Francesca Provenzano[a], Elena Gallia[a], Silvia Ravera[a,1], Carola Torazza[a], Simone Bossi[b], Sara Ferrando[c], Aldamaria Puliti[b,g], Ludo Van Den Bosch[d,e], Giambattista Bonanno[a,f,*], Marco Milanese[a]

[a] Department of Pharmacy, Unit of Pharmacology and Toxicology and Center of Excellence for Biomedical Research, University of Genoa, Genoa, Italy
[b] Department of Neuroscience, Rehabilitation, Ophthalmology, Genetics and Maternal and Child Health, University of Genoa, Genoa, Italy
[c] Department of Earth, Environmental, and Life Science (DISTAV), University of Genoa, Corso Europa 26, I-16132 Genoa, Italy
[d] KU Leuven, Department of Neurosciences, Experimental Neurology, Leuven, Belgium
[e] VIB, Center for Brain & Disease Research, Laboratory of Neurobiology, Leuven, Belgium
[f] IRCCS San Martino Polyclinic Hospital, Genoa, Italy.
[g] UOC Genetica Medica, IRCCS Istituto Giannina Gaslini, Genoa, Italy

ARTICLE INFO

Keywords:
Amyotrophic lateral sclerosis
SOD1^{G93A} mouse
Metabotropic glutamate type 5 receptor
In-vivo
Genetic ablation
Behaviour
Histology, disease progression

ABSTRACT

Amyotrophic lateral sclerosis (ALS) is a fatal neurodegenerative disease due to motor neuron (MN) loss. The mechanisms causing selective MN death are largely unknown, thus prejudicing successful pharmacological treatments. Major causes of MN damage are effects downstream of the abnormal glutamate (Glu) neurotransmission. Group I metabotropic Glu receptors (mGluR1, mGluR5) actively contribute to the excitotoxicity in ALS and represent druggable molecular targets. We previously demonstrated that halving mGluR1 or mGluR5 expression in the widely studied *SOD1^{G93A}* mouse model of ALS had a positive impact on disease onset, clinical progression and survival, as well as on cellular and biochemical parameters altered in ALS. Whereas these effects were similar in female and male mGluR1 heterozygous *SOD1^{G93A}*mice, only male mGluR5 heterozygous *SOD1^{G93A}* mice showed improved motor skills during disease progression. To further validate the role of Group I mGluRs in ALS, we generated in this study mGluR1 or mGluR5 null mice expressing the *SOD1^{G93A}* mutation (*SOD1^{G93A}Grm1$^{crv4/crv4}$* or *SOD1^{G93A}Grm5$^{-/-}$*, respectively). *SOD1^{G93A}Grm1$^{crv4/crv4}$* mice showed early and progressive motor impairments and died even before *SOD1^{G93A}* mice, while *SOD1^{G93A}Grm5$^{-/-}$* mice exhibited delayed disease onset, longer survival, and ameliorated motor skills than *SOD1^{G93A}* mice. No difference between female and male *SOD1^{G93A}Grm5$^{-/-}$* mice were observed. These effects were associated with enhanced MN preservation and decreased astrocytic and microglial activation. Our results strongly support the assumption that constitutively lowering of mGluR5 expression has a positive impact in mice with ALS by counteracting the abnormal Glu transmission and this could be a potentially effective pharmacological target in ALS.

Abbreviations: ALS, amyotrophic lateral sclerosis; MN, motor neuron; Glu, glutamate; mGluR1, metabotropic glutamate receptor type 1; mGluR5, metabotropic glutamate receptor type 5; sALS, sporadic amyotrophic lateral sclerosis; fALS, familial amyotrophic lateral sclerosis; C9orf72, Chromosome 9 Open Reading Frame 72; SOD1, superoxide dismutase type 1; TARDBP, TDP43 43 kDa transactive response-DNA binding protein; FUS/TLS, fused in sarcoma/translocated in liposarcoma; NMDA, *N*-methyl-D-aspartate receptor; AMPA, α-amino-3-hydroxy-5-methyl-4-isoxazole propionate; 3,5-DHPG, (*S*)-3,5-dihydroxyphenylglycine; LTR, long terminal repeat; PCR, polymerase chain reaction; PaGE, paw grip endurance; GSM, Grip-strength Meter; PBS, phosphate-buffered saline; IBA-1, ionized calcium binding adaptor molecule 1; GFAP, glial fibrillary acidic protein; BSA, bovine serum albumin; DAPI, 4′,6-diamidino-2-phenylindole; EDTA, ethylenediamminetetraacetic acid; GAPDH, glyceraldehyde 3-phosphate dehydrogenase; ANOVA, analysis of variance; WB, Western blotting; IF, immunofluorescence

* Corresponding author at: Department of Pharmacy, Viale Cembrano 4, 16148 Genoa, Italy.
E-mail address: bonanno@difar.unige.it (G. Bonanno).
[1] Present address: Department of Experimental Medicine, Unit of Human anatomy, University of Genoa, Genoa, Italy.

https://doi.org/10.1016/j.nbd.2019.05.007
Received 31 January 2019; Received in revised form 19 April 2019; Accepted 11 May 2019
Available online 15 May 2019

1. Introduction

Amyotrophic lateral sclerosis (ALS) is a fatal disease in which cortical and spinal cord motor neurons (MNs) degenerate causing severe and irreversible muscle weakness, wasting and atrophy, with death of patients by respiratory failure within 3–5 years after diagnosis (Eisen, 2009). Approximately, 90% of ALS cases are sporadic (sALS) due to multiple genetic, epigenetic and environmental factors, while about 10% are familial (fALS) (Andersen and Al-Chalabi, 2011), clinically indistinguishable from sALS. Mutations in > 20 genes have been associated with fALS, the most important ones being mutations in Chromosome 9 Open Reading Frame 72 (C9orf72), Superoxide Dismutase type 1 (SOD1), 43 kDa Transactive Response-DNA Binding Protein (TARDBP, TDP43), and Fused in Sarcoma/Translocated in Liposarcoma (FUS/TLS) (Laferriere and Polymenidou, 2015; Alsultan et al., 2016).

The causes of MN death in ALS are not yet completely understood and this has hampered the development of successful pharmacological treatments. Different cellular and molecular mechanisms have been proposed as aetiological causes of ALS. Among others, glutamate(Glu)-mediated excitotoxicity, oxidative stress, neuroinflammation, mitochondrial dysfunction and bioenergetics alterations, protein misfolding and aggregation, impaired axonal transport and dysregulation of RNA signalling have all been suggested as being involved in the disease process (Cleveland et al., 1996; Morrison and Morrison, 1999; Van Den Bosch et al., 2006; Ferraiuolo et al., 2011; Tan et al., 2014; Peters et al., 2015; King et al., 2016). Evidence implicating Glu-mediated excitotoxicity in ALS is mainly based on the presence of elevated levels of extracellular Glu in sporadic and familial ALS patients (Perry et al., 1990; Rothstein et al., 1990; Shaw et al., 1995; Spreux-Varoquaux et al., 2002; Wuolikainen et al., 2011), on the increased Glu transmission in mouse models of ALS, due to the reduced expression of the Glu transporter EAAT2 (Rothstein et al., 1995; Cleveland and Rothstein, 2001), on the abnormal Glu neuronal exocytosis (Milanese et al., 2011; Bonifacino et al., 2016), on the anomalous functioning of postsynaptic Glu receptors at lower MNs (Van Den Bosch et al., 2000; Kuner et al., 2005; Tortarolo et al., 2006), and on the therapeutic use of riluzole, which reduces Glu release (Lazarevic et al., 2018).

Glu is the natural agonist of ionotropic and metabotropic receptors. Ionotropic receptors are the *N*-methyl-D-aspartate (NMDA) receptor, α-amino-3-hydroxy-5-methyl-4-isoxazole propionate (AMPA) and kainate receptors that are assembled as multiple heteromers of different subunits (Conti and Weinberg, 1999; Dingledine et al., 1999). Also, metabotropic Glu receptors (mGluRs) are relevant targets of released Glu (Pin and Acher, 2002; Musante et al., 2008; Nicoletti et al., 2011; Giribaldi et al., 2013; Pittaluga, 2016) and comprise eight receptor subtypes, divided into three groups. Group I mGluRs, which include mGluR1 and mGluR5, are excitatory and their activation produces inositol-1,4,5-trisphosphate and diacylglycerol, resulting in mobilization of intracellular Ca^{2+} and activation of protein kinase C. Group II and III, including the other six mGluRs are inhibitory and negatively coupled to adenylyl cyclase activity (Pin and Duvoisin, 1995; Nicoletti et al., 2011).

A number of reports described that mGluR1 and mGluR5 are overexpressed in the spinal cord of ALS patients and *SOD1*^{G93A} mice (Anneser et al., 1999; Aronica et al., 2001; Valerio et al., 2002; Anneser et al., 2004) and that they contribute to degeneration of neuronal and glial cells (Valerio et al., 2002; Rossi et al., 2008; D'Antoni et al., 2011; Martorana et al., 2012; Battaglia and Bruno, 2018) possibly through a complex mechanism involving inflammation-induced sensitization to neuronal excitotoxicity (Degos et al., 2013). We previously found that exposure to the mGluR1/5 agonist (*S*)-3,5-Dihydroxyphenylglycine (3,5-DHPG) at concentrations > 0.3 μM stimulated Glu release in lumbar spinal cord of both control and *SOD1*^{G93A} mice. At variance, concentrations of 3,5-DHPG ≤0.3 μM increased Glu release in *SOD1*^{G93A} mice only. The Glu release potentiation involved both mGluR1 and mGluR5, while mGluR5 was preferentially involved in the high potency effects of 3,5-DHPG (Giribaldi et al., 2013). More recently, we also demonstrated that halving the expression of mGluR1 or mGluR5 in *SOD1*^{G93A} mice produced delayed disease onset and increased survival, accompanied by improved motor skills and amelioration of a number of histological and biochemical characteristics altered in ALS (Milanese et al., 2014; Bonifacino et al., 2017). Whereas these effects were similar in *SOD1*^{G93A} female and male mGluR1 heterozygous mice (*SOD1*^{G93A}*Grm1*$^{crv4/+}$), only SOD1^{G93A} mGluR5 heterozygous (*SOD1*^{G93A}*Grm5*$^{-/+}$) males showed improved motor skills during disease progression.

To support the translational value of targeting group I mGluRs in ALS, we produced here mice lacking mGluR1 (*SOD1*^{G93A}*Grm1*$^{crv4/crv4}$) or mGluR5 (*SOD1*^{G93A}*Grm5*$^{-/-}$). *SOD1*^{G93A}*Grm1*$^{crv4/crv4}$ mice displayed a negative phenotype that hampered further analysis. Instead, complete knock out of mGluR5 mice had a very positive effect on the phenotype of the *SOD1*^{G93A} mice and exhibited a clinical course that was more favourable than *SOD1*^{G93A}*Grm5*$^{-/+}$ mice. Moreover, motor skills were improved both in female and male *SOD1*^{G93A}*Grm5*$^{-/-}$ mice.

2. Materials and methods

2.1. Animals

B6SJL-Tg(SOD1*G93A)1Gur mice expressing high copy number of mutant human SOD1 with a Gly93Ala substitution (*SOD1*^{G93A} mice; Gurney et al., 1994) were originally obtained from Jackson Laboratories (Bar Harbor, ME, USA). Transgenic male mice were crossed with background-matched B6SJL wild-type females and selective breeding maintains the transgene in the hemizygous state. Transgenic mice are identified analyzing tissue extracts from tail tips as previously described (Stifanese et al., 2010). *Grm1*^{crv4} micecarrying a recessive loss-of-function mutation (*crv4*) in the gene (*Grm1*) coding for mGluR1 were used to obtain *SOD1*^{G93A}*Grm1*$^{crv4/crv4}$ double mutants. The *crv4* mutation is a spontaneous recessive mutation occurred in the BALB/c/Pas inbred strain. It consists of an insertion of a retrotransposon LTR (Long Terminal Repeat) fragment occurred in intron 4 of the *Grm1* gene and causing the disruption of the gene splicing and the absence of the receptor protein (Conti et al., 2006). Affected (*Grm1*$^{crv4/crv4}$) and control (*Grm1*$^{+/+}$) mice are maintained on the same genetic background by intercrossing *Grm1*$^{crv4/+}$ mice. The genotype of *Grm1*^{crv4} mice was identified by real-time polymerase chain reaction (PCR) using specific primers as already reported (Musante et al., 2008). B6.129-Grm5^{tm1Rod}/J, carrying a null mutation for mGluR5 (*Grm5*$^{-/+}$; Lu et al., 1997) were originally obtained from Jackson Laboratories (Bar Harbor, ME, USA). The genotype of *Grm5*$^{-/+}$ mice was identified by PCR using specific primers according to the Jackson Laboratory protocols with minor modifications, as previously described (Bonifacino et al., 2017). *SOD1*^{G93A} male mice (on a mixed C57BL6-SJL background) were bred with *Grm1*$^{crv4/+}$ females (BALB/c background) to generate double-mutants carrying the *Grm1*$^{crv4/+}$ heterozygous mutation and the SOD1*G93A transgene. *SOD1*^{G93A}*Grm1*$^{crv4/+}$ double mutants from the initial crossing were then crossed with *Grm1*$^{crv4/+}$ animals to obtain *SOD1*^{G93A}*Grm1*$^{crv4/crv4}$ mice (Fig. 1). With the same approach, *SOD1*^{G93A} male mice were bred with *Grm5*$^{-/+}$ females to generate *SOD1*^{G93A}*Grm5*$^{-/+}$ double-mutants carrying the *Grm5*$^{-/+}$ heterozygous mutation and the SOD1*G93A transgene. *SOD1*^{G93A}*Grm5*$^{-/+}$double mutants from the initial crossing were then crossed with *Grm5*$^{-/+}$ mice to obtain *SOD1*^{G93A}*Grm5*$^{-/-}$ mice. Animals were housed at constant temperature (22 ± 1 °C) and relative humidity (50%) with a regular 12 h–12 h light cycle (light 7 AM–7 PM), throughout the experiments. Food (type 4RF21) standard diet obtained from Mucedola (Settimo Milanese, Milan, Italy) and water were freely available. All experiments were carried out in accordance with the European Communities Council (EU Directive 114, 2010/63/EU for animal experiments; September 22nd, 2010), with the Italian D.L. n. 26/2014 and were approved by the local Ethical Committee and by the

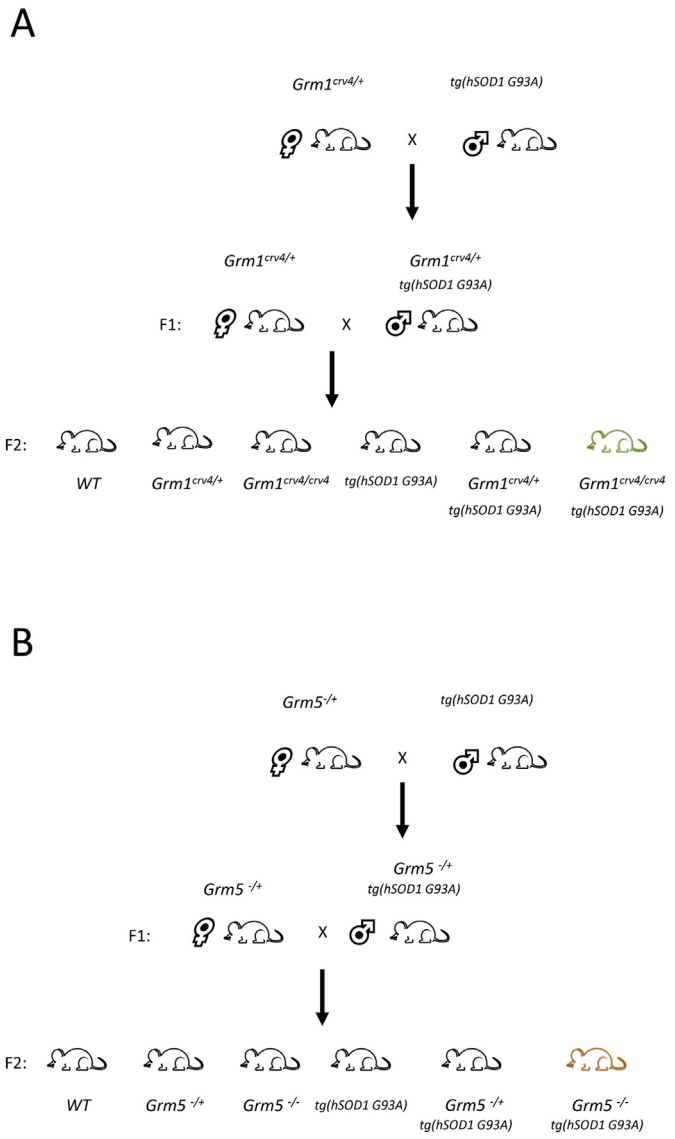

Fig. 1. Schematic representation of animal crossing. Panel (A). *SOD1*^{G93A} male mice were bred with *Grm1*$^{crv4/+}$ females. Four genetically distinct mouse littermates (F1: WT, *Grm1*$^{crv4/+}$, *SOD1*^{G93A}, and *SOD1*^{G93A}*Grm1*$^{crv4/+}$) were obtained (not shown). *SOD1*^{G93A}*Grm1*$^{crv4/+}$ male mice were bred with *Grm1*$^{crv4/+}$ females to generate six genetically distinct mouse littermates (F2: WT, *Grm1*$^{crv4/+}$, *Grm1*$^{crv4/crv4}$, *SOD1*^{G93A}, *SOD1*^{G93A}*Grm1*$^{crv4/+}$, and *SOD1*^{G93A}*Grm1*$^{crv4/crv4}$). *SOD1*^{G93A}*Grm1*$^{crv4/crv4}$ represents the double-mutant mouse carrying both the *Grm1*$^{crv4/crv4}$ homozygous mutation and the SOD1*G93A transgene. Panel (B). *SOD1*^{G93A} male mice were bred with *Grm5*$^{-/+}$ females. Four genetically distinct mouse littermates (F1: WT, *Grm5*$^{-/+}$, *SOD1*^{G93A}, and *SOD1*^{G93A}*Grm5*$^{-/+}$) were obtained (not shown). *SOD1*^{G93A}*Grm5*$^{-/+}$ male mice were bred with *Grm5*$^{-/+}$ females to generate six genetically distinct mouse littermates (F2: WT, *Grm5*$^{-/+}$, *Grm5*$^{-/-}$, *SOD1*^{G93A}, *SOD1*^{G93A}*Grm5*$^{-/+}$, and *SOD1*^{G93A}*Grm5*$^{-/-}$). The *SOD1*^{G93A}*Grm5*$^{-/-}$ is the double-mutant mouse carrying both the *Grm5*$^{-/-}$ homozygous mutation and the SOD1*G93A transgene.

Italian Ministry of Health (Project Authorization No.97/2017-PR). All the animal-involving experiments comply with the ARRIVE guidelines, to minimize animal suffering and to use only the number of animals necessary to produce reliable results. Gender were balanced among the experimental groups to avoid bias due to sex-related intrinsic differences in disease severity. For experimental use animals were killed at a late stage of disease according to a five-point clinical score level, as previously described (Uccelli et al., 2012). A total number of 29 WT, 52 *SOD1*^{G93A}, 8 *SOD1*^{G93A}*Grm1*$^{crv4/crv4}$, 42 *SOD1*^{G93A}*Grm5*$^{-/-}$ and 9 *Grm5*$^{-/-}$ mice were used in this study.

2.2. Survival and motor performance

Body weight: body weight was measured immediately before behavioural tests. Disease onset was defined retrospectively as the time when the body weight was significantly lower than that of control mice (Boillée et al., 2006). *Survival probability*: survival was identified as the time at which mice were unable to right themselves within 20 s when placed on their side. Survival data originated from those animals scored in clinical tests only. Animals used in clinical tests were not used for other experiments. Clinical test registration was started at day 90 and data were recorded three times a week, until death. Tests were performed in randomized order by a blinded observer. *Motor coordination*: mice were rated for disease progression by scoring the Rotarod and the balance beam test performances. *Rotarod test*: the time for which an animal could remain on the rotating cylinder was measured, starting at day 90, using an accelerating Rotarod apparatus (Rota-Rod 7650; Ugo Basile s.r.l., Gemonio,VA, Italy). In this procedure the rod rotation gradually increases in speed from 4 to 40 r.p.m. over the course of 5 min. Before registration animals were trained for 10 days. *Balance beam test*: it consists of 1 m long beam with a 6 mm width upper surface, standing 50 cm above ground. Mice were placed at the starting point and encouraged to cross the beam by means of a black box placed at the end. The number of foot slips while walking along the beam was recorded (Luong et al., 2011). *Motor skills*: mice were rated for disease progression by scoring the extension reflex of hind limbs and the gait. *Extension reflex test*: animals were evaluated by observing the hind limb posture when suspended by the tail. *Gait*: deficits were measured by observing mice in an open field. Motor skills were rated using a 5-point score scale (5, no sign of motor dysfunction; 0, complete impairment) as previously described (Uccelli et al., 2012). *Muscle strength*: mice were rated for disease progression by scoring the grip strength (fore limb muscle strength) and the hanging wire (hind limb paw grip endurance) tests. *Grip strength test*: mice were placed over a base plate in front of a grasping bar fitted to a force sensor, for the automated detection of the animal fore limbs strength. The force transducer has a maximum applicable force of 1500 g, with a resolution 0.1 g (GSM Grip-strength Meter, Ugo Basile s.r.l., Gemonio, VA, Italy). The test was repeated three times per trial and the average value of the mouse grip force (arbitrary units) were registered (Seo et al., 2011). *Hanging wire test*: hind limb grip endurance was measured by placing mice on a cage wire-lid held approximately 50 cm above a cage containing fresh bedding. The wire lid was then cautiously turned upside down and the latency of the animal to go off the grid with both hind limbs was quantified (Alfieri et al., 2014). A 120 s cutoff time was used.

2.3. Histological studies

WT, *Grm5*$^{-/-}$, *SOD1*^{G93A}, and *SOD1*^{G93A}*Grm5*$^{-/-}$ mice (110 days old) were euthanized and spinal cords were post-fixed in 4% paraformaldehyde in phosphate-buffered saline (PBS, pH 7.4) for 24 h. After careful rinses in PBS, the specimen was dehydrated with an increasing ethanol series (80, 90, 95, 100%) and embedded in Paraplast (Sigma-Aldrich, Saint Louis, MO, USA). Longitudinal Paraplast sections (5 µm thick) were cut, rehydrated in a decreasing ethanol series (100, 95, 90, 80%) and washed in PBS. Dewaxed serial sections were incubated overnight in a moist chamber at 4 °C with a rabbit polyclonal antibody against ionized calcium binding adaptor molecule 1 (IBA1, Wako, Osaka, Japan code: 016-20001) or a rabbit polyclonal antibody against glial fibrillary acidic protein (GFAP, Sigma-Aldrich, St. Loius, MO, USA code: G9269). Both antibodies were diluted 1:200 in PBS plus 0.1% bovine serum albumin (BSA). After rinsing in PBS, sections were incubated with Alexa-488-conjugated anti-rabbit antiserum (1:800; Molecular Probes – Thermo Fisher Scientific, Rockford, IL, USA code: #A27034) for 1 h. Sections were then stained with 4′,6-diamidino-2-

phenylindole (DAPI), thoroughly washed in PBS and mounted in a glycerol/PBS (1:1) solution. Sections were examined by an Olympus BX60 epifluorescence microscope (Ravera et al., 2016). To evaluate the number and the morphology of MNs, fixed section series were also stained using haematoxylin and eosin (Cardiff et al., 2014). MNs were selected and counted based on diameters > 25 μm.

2.4. Protein expression

Spinal cords of 110 days old WT, *Grm5*$^{-/-}$, *SOD1*^{G93A}, and *SOD1*^{G93A}*Grm5*$^{-/-}$ mice were dissected and homogenized in lysis buffer (10 mM Tris, pH 8.8, 20% glycerol, 2% sodium dodecyl sulphate (SDS), 0.1 mM ethylenediamminetetraacetic acid (EDTA), 5% β-mercaptoethanol). Protein concentration was determined according to Bradford (1976) using bovine serum albumin (Sigma-Aldrich, St Louis, Missouri, USA) as a standard. Appropriate amount (10–15 μg) of total proteins were separated by SDS-polyacrylamide gel electrophoresis using 4–15% or 4–20% precast gels (Bio-Rad, Segrate, MI, Italy). Protein electro-blotting was monitored by naphthol blue staining of gels (Sigma-Aldrich, St Louis, MO, USA). Membranes were then incubated with a mouse monoclonal anti-mGluR1 antibody (1:2500; BD Biosciences, San Jose, CA, USA; code: 610964), a rabbit polyclonal anti-mGluR5 (1:10000, Epitomics, Burlingame, CA, USA; code : 2237–1), anti-GFAP mouse monoclonal antibody (1:1000, Sigma-Aldrich, St. Loius, MO, USA code: G9269) or anti-IBA1 rabbit polyclonal antibody (1:1000, Wako, Osaka, Japan code: 016–,20001) and with a mouse monoclonal anti-glyceraldehyde-3-phosphate dehydrogenase (GAPDH) antibody (1:10000; Millipore, Billerica, MA, USA; code: MAB374). After incubation with appropriate peroxidase-coupled secondary antibodies, protein bands were detected by a Western blotting (WB) detection system (ECL Advance™; Amersham Biosciences, Piscataway, NJ, USA). Bands were detected and analyzed for density using an enhanced chemiluminescence system (Alliance 6.7 WL 20 M, UVITEC, Cambridge, UK) and UV1D software (UVITEC). Bands of interest were normalized for GAPDH level in the same membrane. The concentration of proteins felt in the linear portion of the curve.

2.5. Statistics

Data are expressed as mean ± s.e.m. and p value < .05 was considered significant. The Kaplan–Meier plot was used to evaluate survival probability and cumulative curves were compared using the log-rank test. All the data sets passed normality test and equal variance test. One-tail Student *t*-test to compare two mean populations and one-way ANOVA followed by Bonferroni post hoc tests for multiple comparisons were used. Statistical analyses were performed by means of SigmaStat 3.5 (Systat Software, Inc., San Jose, CA, USA).

3. Results

3.1. Generation of *SOD1*^{G93A}*Grm1*$^{crv4/crv4}$ and *SOD1*^{G93A}*Grm5*$^{-/-}$ mice

To obtain mice expressing the human G93A-mutated SOD1 and lacking mGluR1, we crossed *SOD1*^{G93A} transgenic mice with the *Grm1*$^{crv4/+}$ mouse line, carrying a recessive loss-of-function mutation (*crv4*) in the gene (*Grm1*) coding for mGluR1 (Conti et al., 2006). Double transgenic heterozygous mice from the first breeding were again crossed with the heterozygous *Grm1*$^{crv4/+}$ mouse line to obtain homozygous double mutants (Fig. 1, panel A). WT, *Grm1*$^{crv4/+}$, *Grm1*$^{crv4/crv4}$, *SOD1*^{G93A}, *SOD1*^{G93A}*Grm1*$^{crv4/+}$, and *SOD1*^{G93A}*Grm1*$^{crv4/crv4}$ were all born at the expected Mendelian ratio and were indistinguishable from WT littermates at birth, except for *SOD1*^{G93A}*Grm1*$^{crv4/crv4}$, that were characterized by reduced dimensions at birth and showed motor alteration typical of an ataxic phenotype during growth. Remarkably, *Grm1*$^{crv4/crv4}$ mice showed almost the same phenotype. These neurological characteristics hampered assessing disease progression and motor abilities in *SOD1*^{G93A}*Grm1*$^{crv4/crv4}$ mice. In addition, these mice survived even less than *SOD1*^{G93A} mice (Table 1). Therefore, we abandoned the studies with *SOD1*^{G93A}*Grm1*$^{crv4/crv4}$ mice.

Table 1
SOD1^{G93A}*Grm1*$^{crv4/crv4}$ mice survival.

SOD1^{G93A}Grm1$^{crv4/crv4}$ mice	
Gender (ID)	Survival (days)
Male #1	105
Male #2	28
Male #3	121
Male #4	102
Female #1	103
Female #2	103
Female #3	35
Female #4	111
Female #5	30

Similarly, we crossed *SOD1*^{G93A} mice and *Grm5*$^{-/+}$ mice, heterozygous for mGluR5, obtaining a F1 generation carrying the G93A mutation but lacking half of mGluR5 (*SOD1*^{G93A}*Grm5*$^{-/+}$). *SOD1*^{G93A}*Grm5*$^{+/-}$ did not show specific signs at birth. As reported previously, they developed a favourable phenotype during disease progression when compared to *SOD1*^{G93A} mice, although males only were better performant in motor skill tests (Bonifacino et al., 2017). Double transgenic heterozygous mice from the first breeding were again crossed with the heterozygous *Grm5*$^{-/+}$ mouse line to obtain homozygous double-mutants (Fig. 1, panel B). WT, *Grm5*$^{-/+}$, *Grm5*$^{-/-}$, *SOD1*^{G93A}, *SOD1*^{G93A}*Grm5*$^{-/+}$, and *SOD1*^{G93A}*Grm5*$^{-/-}$ mice were all born at the expected Mendelian ratio and were all indistinguishable from WT littermates at birth.

To verify the impact of the genetic manipulation on receptor expression, spinal cord lysates of WT, *Grm5*$^{-/-}$, *SOD1*^{G93A}, and *SOD1*^{G93A}*Grm5*$^{-/-}$ mice were analyzed for mGluR1 and mGluR5 expression by immunoblot (Fig. 2A). The analysis showed that mGluR5 was over-expressed in *SOD1*^{G93A} mice compared to WT (about 40% increase; $p < .05$, $F_{(3,8)} = 89.792$) and that its expression was indeed absent in *Grm5*$^{-/-}$ and in *SOD1*^{G93A}*Grm5*$^{-/-}$ mice (Fig. 2B). The mGluR1 expression did not change significantly in the four mouse lines (Fig. 2C).

3.2. Disease onset is delayed and survival is increased in *SOD1*^{G93A}*Grm5*$^{-/-}$ mice

SOD1^{G93A} and *SOD1*^{G93A}*Grm5*$^{-/-}$ mice showed a significant decrease in body weight compared to WT mice. This decrease in body weight became significant starting around day 118 of life in male *SOD1*^{G93A} mice ($p < .05$, $t_{(23)} = -2.256$) and around day 132 in male *SOD1*^{G93A}*Grm5*$^{-/-}$ mice ($p < .01$, $t_{(18)} = -3.288$) (Fig. 3A). As to female *SOD1*^{G93A} and *SOD1*^{G93A}*Grm5*$^{-/-}$ mice, the decrease of body weight became significant starting around day 111 ($p < .05$, $t_{(15)} = -2.230$) and day 120 ($p < .05$, $t_{(15)} = -2.448$), respectively (Fig. 3B). The weight decrease was always less pronounced in *SOD1*^{G93A}*Grm5*$^{-/-}$ compared to *SOD1*^{G93A} mice.

This shift in weight loss in *SOD1*^{G93A}*Grm5*$^{-/-}$ mice, which has been linked to the appearance of symptoms (Boillée et al., 2006), suggests that eliminating mGluR5 in *SOD1*^{G93A} mice significantly delayed the disease onset.

Abolishing mGluR5 prolonged the life span of the *SOD1*^{G93A}*Grm5*$^{-/-}$ double-mutant mice compared to *SOD1*^{G93A} mice. The Kaplan-Meier curve reported in Fig. 4A shows a significant ($p < .001$) survival amelioration in mixed male and female *SOD1*^{G93A}*Grm5*$^{-/-}$respect to *SOD1*^{G93A} mice. The average survival was 131.3 ± 2.5 days in the case of *SOD1*^{G93A} mice and 153.2 ± 4.2 days in the case of *SOD1*^{G93A}*Grm5*$^{-/-}$ mice ($p < .001$; $t_{(37)} = 4.880$). Since we previously experienced gender differences in mGluR5-lacking

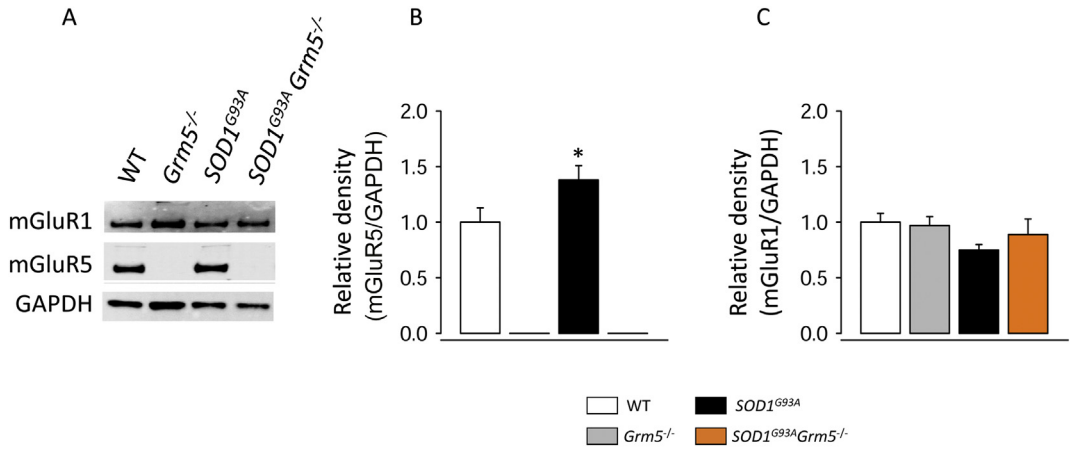

Fig. 2. Expression of mGluR1 and mGluR5 in spinal cord of WT, *Grm5*$^{-/-}$, *SOD1*^{G93A}, and *SOD1*^{G93A}*Grm5*$^{-/-}$ mice. The amount of mGluR5 (B) and mGluR1 (C) in spinal cord homogenates was quantified by SDS-PAGE and WB. Mouse anti-mGluR1 monoclonal antibody or rabbit anti-mGluR5 polyclonal antibody was used. mGluR1 and mGluR5 bands were normalized for GAPDH and are shown as relative to the WT genotype. Representative immunoreactive bands (A) and quantitative analysis are reported. Data are Means ± s.e.m. of 3 independent experiments run in triplicate (3 mice per group, 3 loading per mouse; 2 male 1 female in each group of WT, *SOD1*^{G93A}, *Grm5*$^{-/-}$, and *SOD1*^{G93A}*Grm5*$^{-/-}$ mice). *$p < .05$ and **$p < .001$ vs. WT and $^{\#}p < .001$ vs. *SOD1*^{G93A} (One-way ANOVA followed by Bonferroni post-hoc tests).

heterozygous *SOD1*^{G93A} mice (Bonifacino et al., 2017), we looked also at the survival and behavioural abilities of male and female mice, separately. When survival was analyzed in male mice, a more pronounced shift of *SOD1*^{G93A}*Grm5*$^{-/-}$ mouse Kaplan-Meier curve was observed. The Kaplan-Meier survival probability curves of male *SOD1*^{G93A}*Grm5*$^{-/-}$ and *SOD1*^{G93A} mice were significantly different ($p < .001$) and the shift was more pronounced than in mixed sexes (Fig. 4B). The mean survival age was 129.2 ± 3.2 days in the case of male *SOD1*^{G93A}, while it was 158.4 ± 6.6 days in the case of male *SOD1*^{G93A}*Grm5*$^{-/-}$ mice ($p < .001$, $t_{(23)} = 4.401$). The mean survival age of female *SOD1*^{G93A} mice was 129.6 ± 1.9 days while it was 145.9 ± 2.7 days in female *SOD1*^{G93A}*Grm5*$^{-/-}$ mice ($p < .001$, $t_{(12)} = 4.959$). Although less pronounced, also the shift of the Kaplan-Meyer survival probability curve of female *SOD1*^{G93A}*Grm5*$^{-/-}$mice was significantly different ($p < .001$) from that of *SOD1*^{G93A} mice (Fig. 4C).

From these results we conclude that the total ablation of mGluR5 increases survival both in male and female *SOD1*^{G93A}*Grm5*$^{-/-}$ mice.

3.3. Behavioural performances are improved in *SOD1*^{G93A}*Grm5*$^{-/-}$ mice

To assess the effects of abolishing mGluR5 expression in *SOD1*^{G93A} mice on the decay of behavioural performances during disease progression, we analyzed motor coordination, motor skills and muscle parameters strength in *SOD1*^{G93A} and *SOD1*^{G93A}*Grm5*$^{-/-}$ mice. Motor coordination was evaluated by Rotarod and balance beam tests and motor skills were assessed by monitoring hind limb extension reflex and gait. The muscle strength was determined by hanging wire and a grip strength meter tests. As expected, the performance of *SOD1*^{G93A} mice for these tasks was the same as that of WT mice (not shown in the figures) until around day 80, subsequently it rapidly worsened.

In this later phase, *SOD1*^{G93A}*Grm5*$^{-/-}$ mice performed significantly better than *SOD1*^{G93A} mice for the Rotarod task, meaning that their age-dependent deterioration was much slower (Fig. 5A). We then analyzed the sex contribution to the above results. Motor coordination of *SOD1*^{G93A}*Grm5*$^{-/-}$ mice was significantly increased both in male

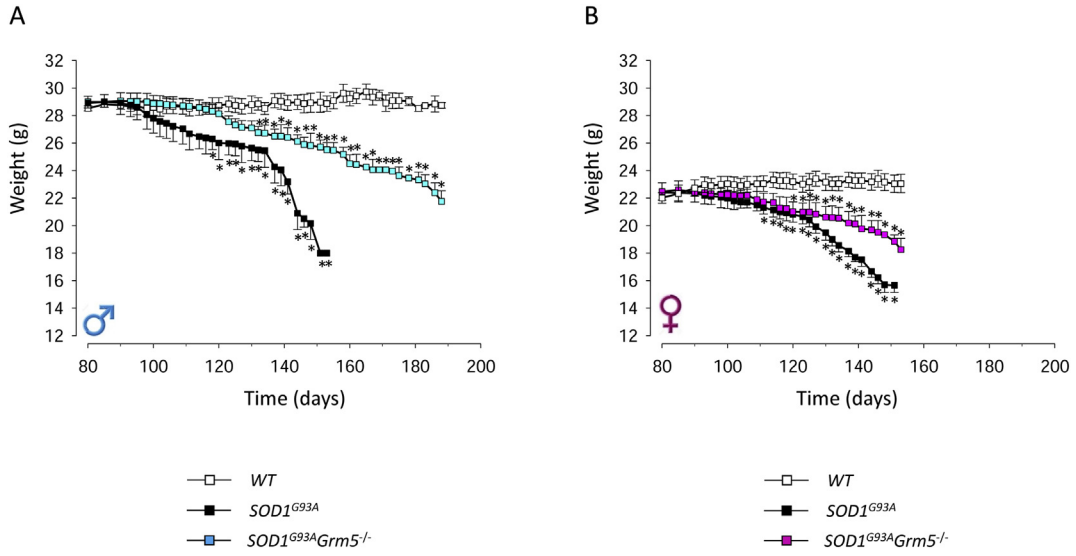

Fig. 3. Body weight in *SOD1*^{G93A} and *SOD1*^{G93A}*Grm5*$^{-/-}$ mice. Body weight was measured immediately before behavioural tests in WT, *SOD1*^{G93A}, and *SOD1*^{G93A}*Grm5*$^{-/-}$ male (A) and female (B) mice as a mark of disease onset. Data are means ± s.e.m. of 10 WT, 15 *SOD1*^{G93A}, and 10 *SOD1*^{G93A}*Grm5*$^{-/-}$ males per group (A) and of 10 WT, 7 *SOD1*^{G93A}, and 7 *SOD1*^{G93A}*Grm5*$^{-/-}$ females per group (B). The first day in which the body weight of *SOD1*^{G93A} or of *SOD1*^{G93A}*Grm5*$^{-/-}$ mice was statistically different from that of WT mice were registered as an index of clinical onset. *$p < .05$ at least (one-tail Student *t*-test).

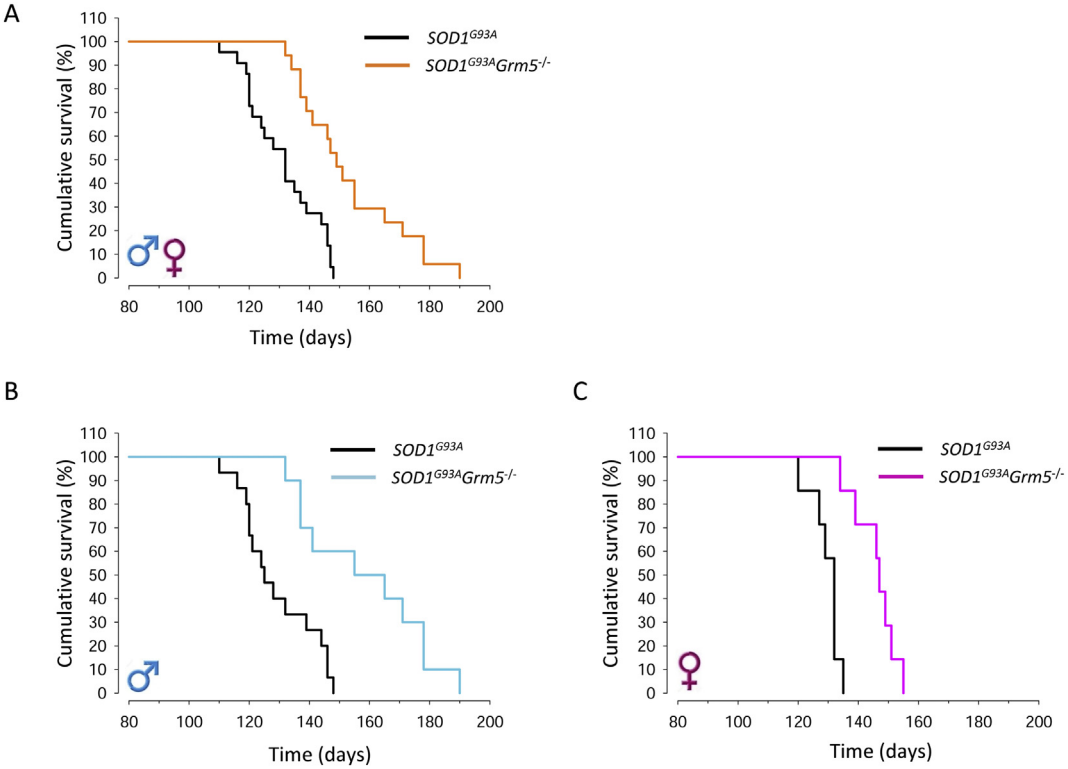

Fig. 4. Survival probability in $SOD1^{G93A}$ and $SOD1^{G93A}Grm5^{-/-}$ mice. Kaplan-Meyer analysis was used to determine the survival probability differences between $SOD1^{G93A}$ and $SOD1^{G93A}Grm5^{-/-}$ in male + female (A), male (B), and female (C) mice. Survival time was assumed as the time when animals were unable to right itself within 20 s when placed on their side. Data are means ± s.e.m. of 15 $SOD1^{G93A}$ and 10 $SOD1^{G93A}Grm5^{-/-}$ males, and of 7 $SOD1^{G93A}$ and 7 $SOD1^{G93A}Grm5^{-/-}$ females. The difference between Kaplan-Meyer curves was significant at $p < .001$ in A, B, and C panels (Log-rank test).

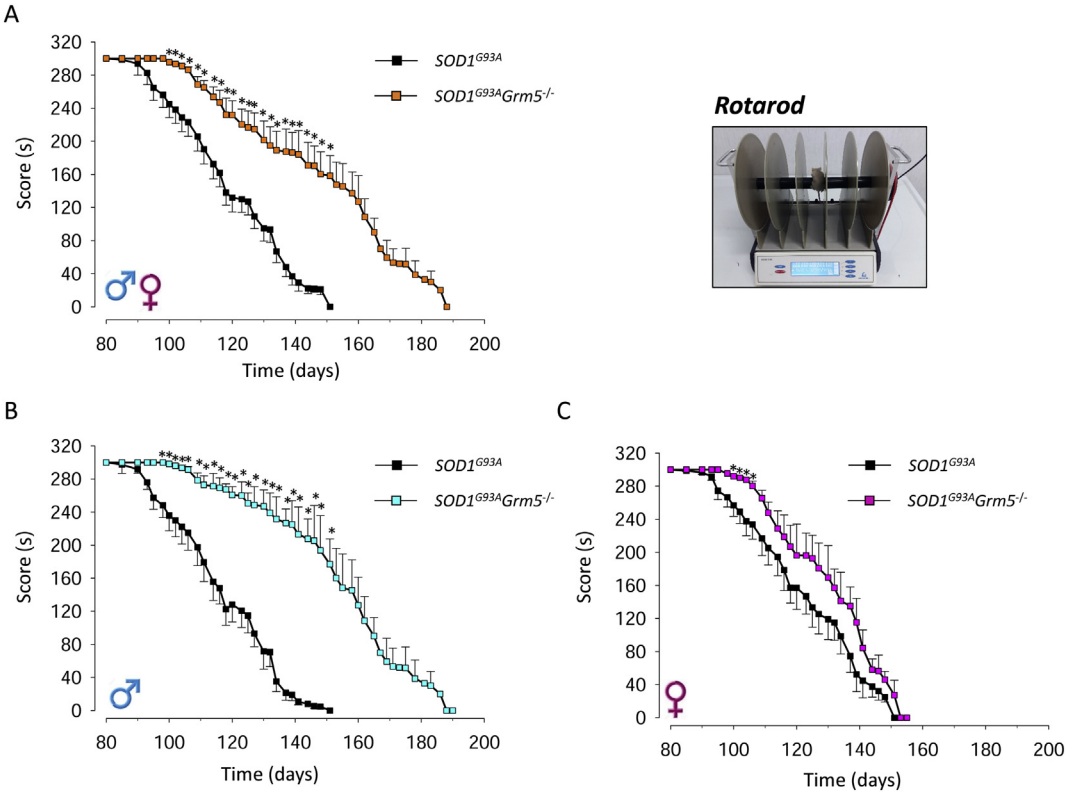

Fig. 5. Rotarod test in $SOD1^{G93A}$ and $SOD1^{G93A}Grm5^{-/-}$ mice. The Rotarod test was used to determine motor coordination differences during the disease progression between $SOD1^{G93A}$ and $SOD1^{G93A}Grm5^{-/-}$ in male + female (A), male (B), and female (C) mice. Animals were tested 3 days a week starting on day 90. The Rotarod speed was increased from 4 to 40 rpm in 5 min and falling off time was recorded. Data are means ± s.e.m. of 12 $SOD1^{G93A}$ and 9 $SOD1^{G93A}Grm5^{-/-}$ males and of 12 $SOD1^{G93A}$ and 7 $SOD1^{G93A}Grm5^{-/-}$ females. $*p < .05$ at least (one-tail Student *t*-test).

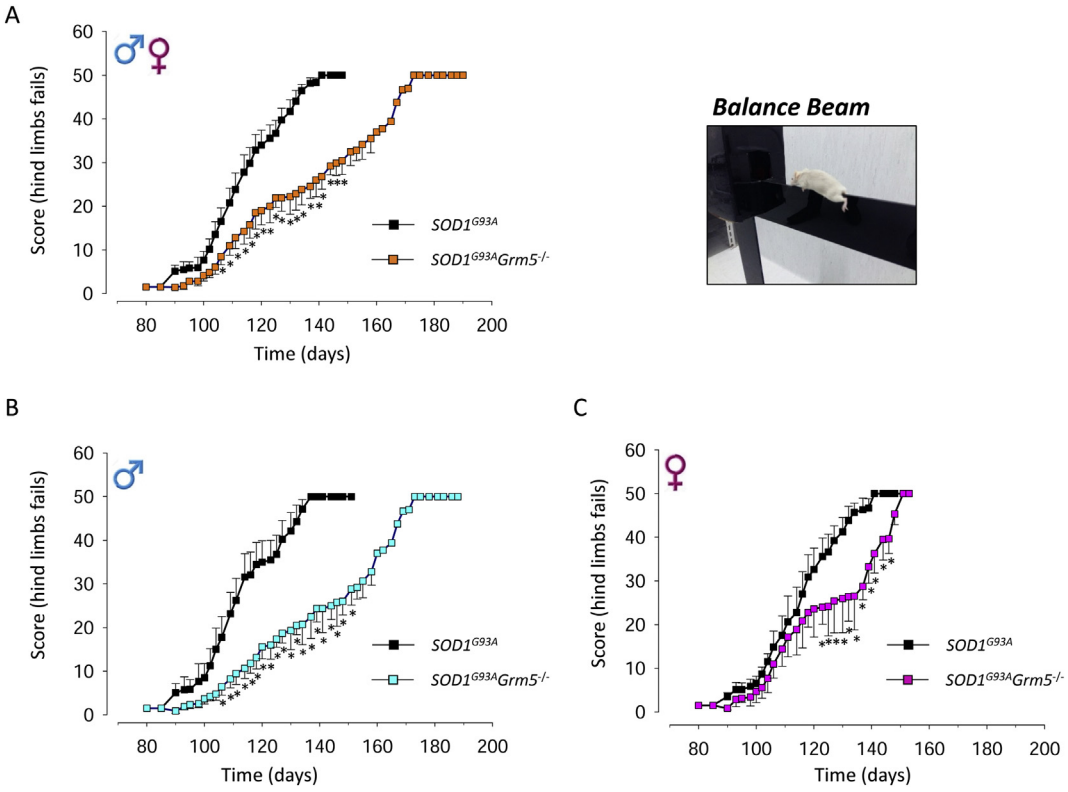

Fig. 6. Balance beam test in $SOD1^{G93A}$ and $SOD1^{G93A}Grm5^{-/-}$ mice. The balance beam test was used to determine motor coordination differences during the disease progression between $SOD1^{G93A}$ and $SOD1^{G93A}Grm5^{-/-}$ in male + female (A), male (B), and female (C) mice. Animals were tested 3 days a week starting on day 90. The number of hind limbs fails during crossing the beam was registered. Data are means ± s.e.m. of 12 $SOD1^{G93A}$ and 9 $SOD1^{G93A}Grm5^{-/-}$ males and of 12 $SOD1^{G93A}$ and 7 $SOD1^{G93A}Grm5^{-/-}$ females. *$p < .05$ at least (one-tail Student t-test).

(Fig. 5B) and female (Fig. 5C) mice, although males exhibited a more pronounced shift of the curve.

Results of the balance beam task are reported in Fig. 6A and show that the number of fails while crossing the beam were lower in $SOD1^{G93A}Grm5^{-/-}$ mice when compared to age-matched $SOD1^{G93A}$ mice. The fails vs. age curve was significantly shifted to the right both in male and female $SOD1^{G93A}Grm5^{-/-}$ mice, however male $SOD1^{G93A}Grm5^{-/-}$ mice (Fig. 6B) performed better than females (Fig. 6C).

$SOD1^{G93A}Grm5^{-/-}$ mice performed significantly better than $SOD1^{G93A}$ mice also in the motor skill tests. In the extension reflex task, $SOD1^{G93A}Grm5^{-/-}$ mice obtained a better score than $SOD1^{G93A}$ (Fig. 7A) and again males (Fig. 7B) were better than females (Fig. 7C).

Gait task in an open field was monitored in $SOD1^{G93A}Grm5^{-/-}$ mice. These mice always obtained a better score than $SOD1^{G93A}$ mice (Fig. 8A) and again males performed better than females (Fig. 8B and C, respectively).

Similarly, $SOD1^{G93A}Grm5^{-/-}$ mice performed significantly better than $SOD1^{G93A}$ mice in the hanging wire test, measuring hind limbs muscle strength test. The analysis revealed an improvement in $SOD1^{G93A}Grm5^{-/-}$mice when compared to $SOD1^{G93A}$ mice (Fig. 9A). Differently from above, the amelioration observed in male (Fig. 9B) and females (Fig. 9C) were similar.

Finally, the grip strength meter, measuring the fore limb muscle strength, indicated that the fore limb force was increased in $SOD1^{G93A}Grm5^{-/-}$ vs. $SOD1^{G93A}$ mice (Fig. 10A). This effect was evident in male $SOD1^{G93A}Grm5^{-/-}$ mice while it was only barely detectable in females (Fig. 10B and C, respectively).

In conclusion, all the behavioural tests show that ablating mGluR5 in $SOD1^{G93A}$ mice resulted in a remarkable slowing down of the progression of the ALS phenotype both in female and male $SOD1^{G93A}Grm5^{-/-}$ mice.

3.4. Motor neurons are preserved in $SOD1^{G93A}Grm5^{-/-}$ mice

Degeneration of MNs in ventral horns of the spinal cord is a well-documented feature of ALS progression (Shaw and Eggett, 2000). MN number was assessed in haematoxylin and eosin-stained lumbar spinal cord sections (L4/L5) of 110 days-old WT, $Grm5^{-/-}$, $SOD1^{G93A}$, and $SOD1^{G93A}Grm5^{-/-}$ mice. Comparable histological features and MN occurrence were observed in WT and $Grm5^{-/-}$ mice. In contrast, $SOD1^{G93A}$ mice showed tissue damage associated with severe neuronal loss and $SOD1^{G93A}Grm5^{-/-}$ mice displayed mixed histological features (Fig. 11A). The number of MNs in the ventrolateral horn of spinal cord was 48.00 ± 1.29, 49.17 ± 1.19, 20.28 ± 1.37, and 28.43 ± 0.99 in WT, $Grm5^{-/-}$, $SOD1^{G93A}$, and $SOD1^{G93A}Grm5^{-/-}$ mice, respectively (Fig. 11B), indicating that the number of MNs was significantly increased ($p < .01$, $F_{(3,8)} = 139.457$) in $SOD1^{G93A}Grm5^{-/-}$ double-mutant mice at an advanced stage of the disease respect to age-matched $SOD1^{G93A}$ mice.

These results confirm that abolishing mGluR5 in $SOD1^{G93A}$ mice protected MNs, which is in line with the delay of disease onset, the amelioration of disease progression and the augmentation of survival reported above.

3.5. Astrogliosis and microgliosis are reduced in $SOD1^{G93A}Grm5^{-/-}$ mice

Astrocytic and microglial activation are key features of ALS (Rossi et al., 2008; Lasiene and Yamanaka, 2011). We investigated the expression of GFAP and IBA-1 as markers for reactive astrocytes and microglia, respectively, in WT, $Grm5^{-/-}$, $SOD1^{G93A}$, and $SOD1^{G93A}Grm5^{-/-}$ mice by immunohistochemistry and WB.

Fig. 12A shows representative confocal microscopy images of GFAP expression in the ventral horns of lumbar spinal cord slices obtained from the four mouse lines. The quantitative analysis showed that the

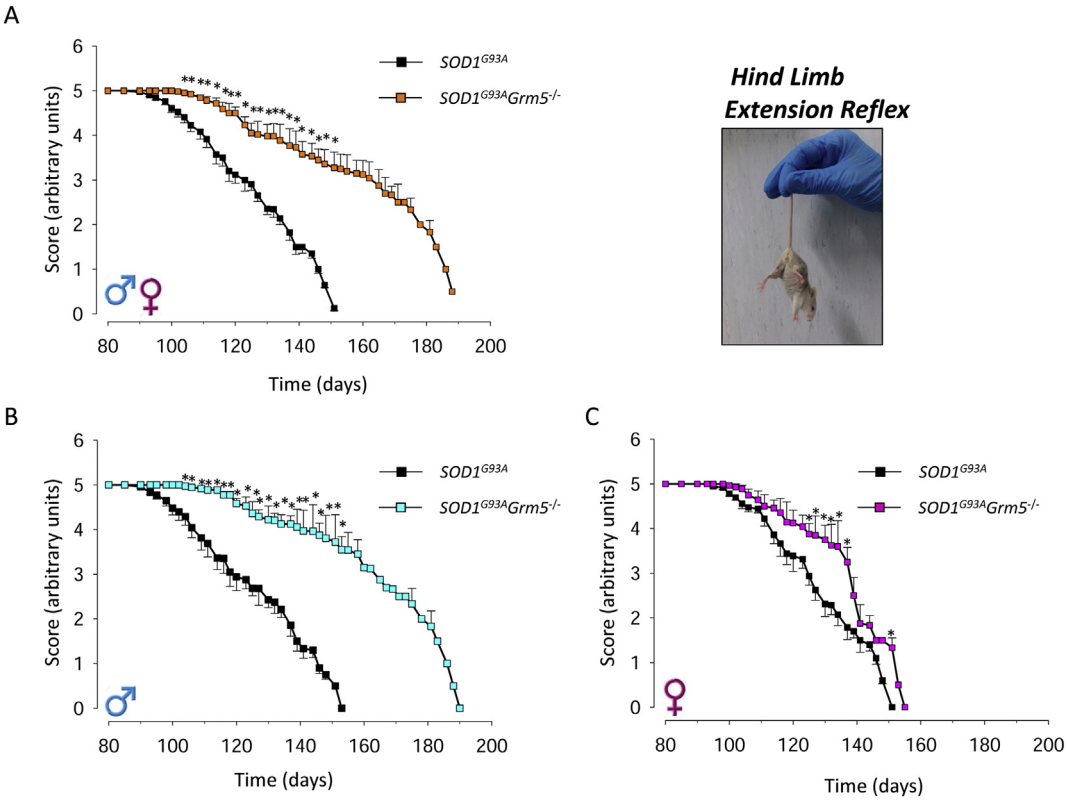

Fig. 7. Hind limbs extension reflex test in $SOD1^{G93A}$ and $SOD1^{G93A}Grm5^{-/-}$ mice. The hind limb extension reflex test was analyzed to determine motor skill differences during the disease progression between $SOD1^{G93A}$ and $SOD1^{G93A}Grm5^{-/-}$ in male + female (A), male (B), and female (C) mice. Animals were tested 3 days a week starting on day 90. Animals were suspended by tail and a 0–5 scale was used to score hind limb postures. Data are means ± s.e.m. of 12 $SOD1^{G93A}$ and 9 $SOD1^{G93A}Grm5^{-/-}$ males and of 12 $SOD1^{G93A}$ and 7 $SOD1^{G93A}Grm5^{-/-}$ females. *$p < .05$ at least (one-tail Student *t*-test).

expression of GFAP was comparable between WT and $Grm5^{-/-}$ mice but it was significantly higher in $SOD1^{G93A}$ compared to WT mice ($p < .001$, $F_{(3,8)} = 45.513$). Interestingly, in $SOD1^{G93A}Grm5^{-/-}$ mice, GFAP fluorescence was reduced vs. $SOD1^{G93A}$ mice ($p < .01$, $F_{(3,8)} = 45.513$) (Fig. 12B). Comparable results were obtained analyzing the GFAP expression in WT, $Grm5^{-/-}$, $SOD1^{G93A}$, and $SOD1^{G93A}Grm5^{-/-}$ mice by SDS-PAGE and WB. Again GFAP expression was increased in $SOD1^{G93A}$ vs. WT mice ($p < .001$, $F_{(3,8)} = 20.663$) and this overexpression was reduced in $SOD1^{G93A}Grm5^{-/-}$ mice ($p < .05$, $F_{(3,8)} = 20.663$). GFAP expression in $SOD1^{G93A}Grm5^{-/-}$ mice did not differ significantly from control $Grm5^{-/-}$ mice. See Fig. 12C for a representative immunoblot and Fig. 12D for quantitative analyses.

The expression of the reactive microglial marker IBA-1, investigated by confocal microscopy, was similar in WT and $Grm5^{-/-}$ mice and, as expected, it was overexpressed in $SOD1^{G93A}$ compared to WT mice ($p < .001$, $F_{(3,8)} = 306.215$). IBA-1 overexpression was significantly reduced in $SOD1^{G93A}Grm5^{-/-}$ mice ($p < .001$, $F_{(3,8)} = 306.215$) (Fig. 13A, B). WB analysis in WT, $Grm5^{-/-}$, $SOD1^{G93A}$, and $SOD1^{G93A}Grm5^{-/-}$ homogenates produced comparable results ($p < .001$, $F_{(3,8)} = 84.391$, $SOD1^{G93A}$ vs. WT mice; $p < .001$, $F_{(3,8)} = 20.663$, $SOD1^{G93A}Grm5^{-/-}$ vs. $SOD1^{G93A}$ mice; $p < .001$, $F_{(3,8)} = 20.663$, $SOD1^{G93A}Grm5^{-/-}$ vs. $Grm5^{-/-}$mice) (Fig. 13C, D).

We conclude that ablating mGluR5 in SOD^{G93A} mice reduced astrocytic and microglial activation, possibly creating a more beneficial extracellular milieu for MNs.

4. Discussion

A wealth of data supports the view that altered excitatory transmission plays a substantial role in neuronal and non-neuronal cell damage in ALS. One major argument is represented by the elevation of Glu concentration in plasma and cerebrospinal fluid of animal models of the disease and of ALS patients. In previous work, we have demonstrated that these excessive extracellular Glu can be supported by abnormal exocytotic and non-exocytotic release of the excitatory amino acid from glutamatergic nerve terminals and glial peri-synaptic processes in the spinal cord of $SOD1^{G93A}$ mice (Raiteri et al., 2003; Raiteri et al., 2004; Milanese et al., 2010; Milanese et al., 2011; Milanese et al., 2015; Bonifacino et al., 2016) and that activation of presynaptic mGluR1 and mGluR5 autoreceptors at spinal cord glutamatergic nerve terminals also resulted in abnormal stimulation of Glu release in $SOD1^{G93A}$ mice (Giribaldi et al., 2013). Our results are in line with previous studies indicating that these receptors are implicated in ALS and that they are aberrantly expressed in neuronal and glial cells during disease progression (Aronica et al., 2001; Valerio et al., 2002; Anneser et al., 2004; Rossi et al., 2008; D'Antoni et al., 2011; Martorana et al., 2012). To reinforce this hypothesis, we demonstrated that halving the expression of mGluR1 or mGluR5 in the $SOD1^{G93A}$ mouse significantly delayed the disease on-set, increased the survival probability, improved spinal MN preservation, reduced astrogliosis and microgliosis, normalized the abnormal Glu release accompanied by improved motor functions (Milanese et al., 2014; Bonifacino et al., 2017). Intriguingly and at variance of the results obtained in $SOD1^{G93A}Grm1^{crv4/+}$, only male $SOD1^{G93A}Grm5^{-/+}$ mice performed better than $SOD1^{G93A}$ mice in motor tasks during disease progression (Bonifacino et al., 2017).

In this study, we investigated whether knocking out mGluR1 or mGluR5 could further improve the positive effects obtained previously with heterozygous mice. Unfortunately, the $SOD1^{G93A}Grm1^{crv4/crv4}$ double-mutants, knockout for mGluR1, showed a very negative phenotype characterized by serious ataxic symptoms, that were also present in founder $Grm1^{crv4/crv4}$ mice (Rossi et al., 2013), possibly due to the ablation of this receptor at the cerebellar level where it plays a key role in the regulation of motor functions (Swanson and Kalivas, 2000;

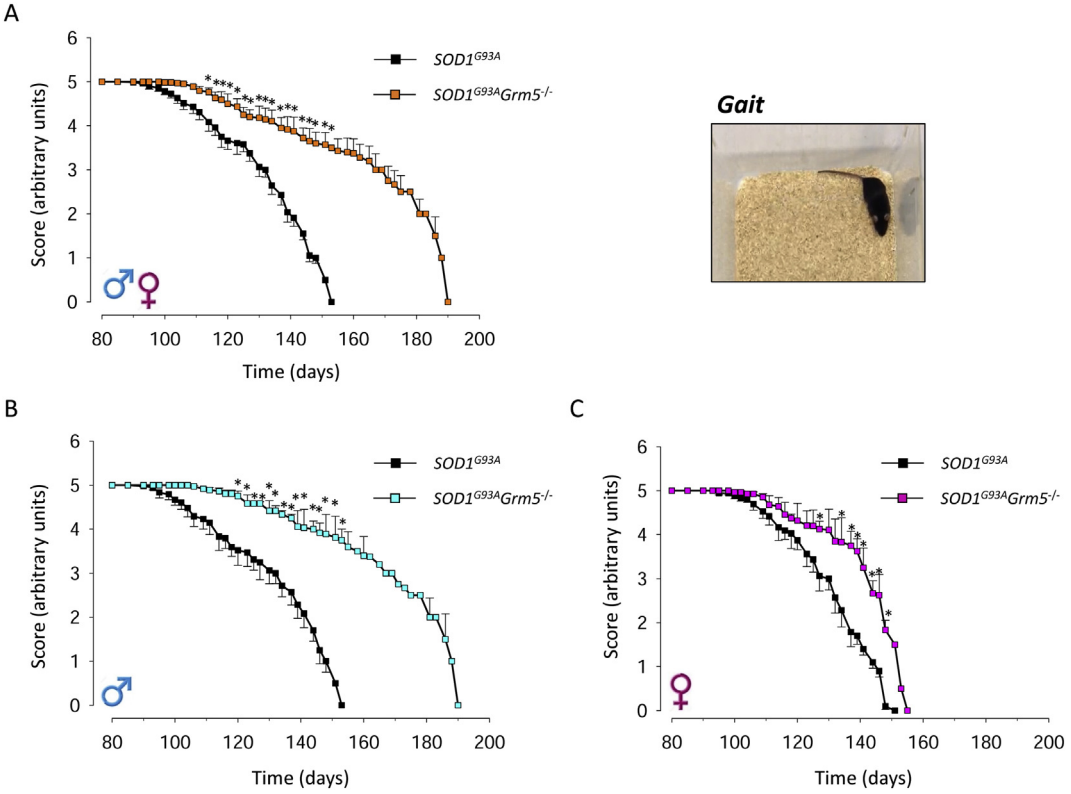

Fig. 8. Gait test in $SOD1^{G93A}$ and $SOD1^{G93A}Grm5^{-/-}$ mice. The gait test was used to determine motor skill differences during the disease progression between $SOD1^{G93A}$ and $SOD1^{G93A}Grm5^{-/-}$ in male + female (A), male (B), and female (C) mice. Animals were tested 3 days a week starting on day 90. Animals were allowed to move in an open space and a 0–5 scale was used to score walk impairment. Data are means ± s.e.m. of 12 $SOD1^{G93A}$ and 9 $SOD1^{G93A}Grm5^{-/-}$ males and of 12 $SOD1^{G93A}$ and 7 $SOD1^{G93A}Grm5^{-/-}$ females. *$p < .05$ at least (one-tail Student *t*-test).

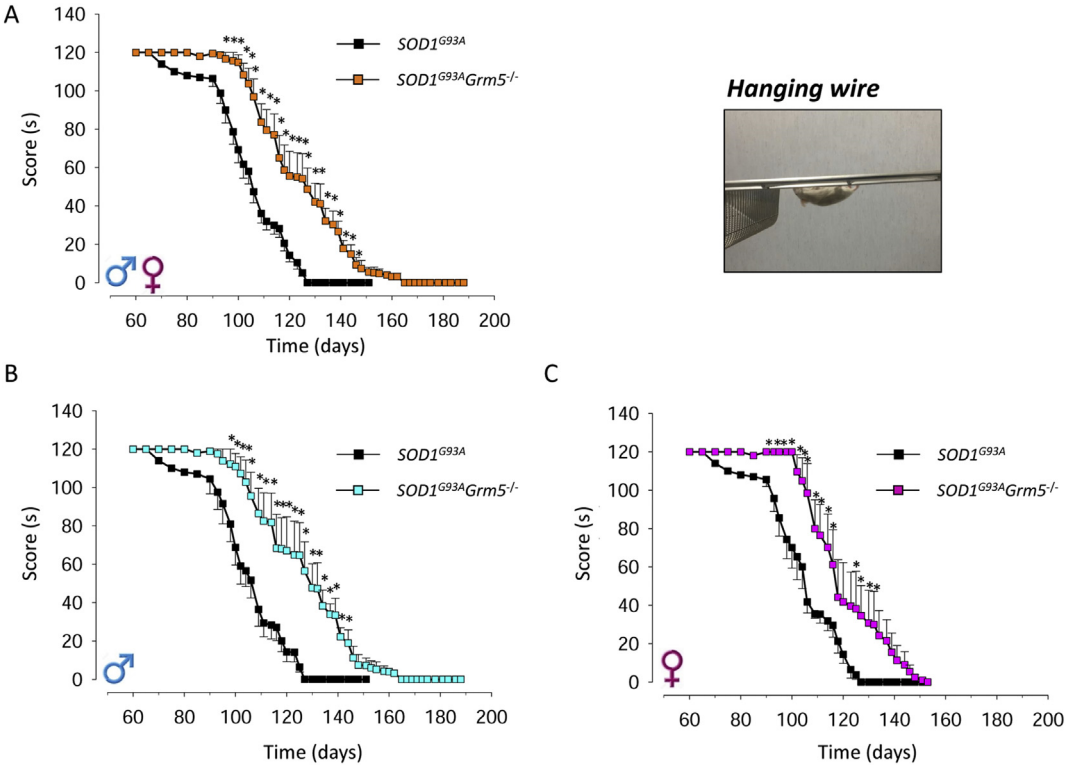

Fig. 9. Hanging wire test in $SOD1^{G93A}$ and $SOD1^{G93A}Grm5^{-/-}$ mice. The wire hang test was used to determine hind limb muscle strength differences during the disease progression between $SOD1^{G93A}$ and $SOD1^{G93A}Grm5^{-/-}$ in male + female (A), male (B), and female (C) mice. Animals were tested 3 days a week starting on day 90. Animals were placed on a grid which was turned upside down and the hind limb detach time was recorded. Data are means ± s.e.m. of 12 $SOD1^{G93A}$ and 9 $SOD1^{G93A}Grm5^{-/-}$ males and of 12 $SOD1^{G93A}$ and 7 $SOD1^{G93A}Grm5^{-/-}$ females. *$p < .05$ at least (one-tail Student *t*-test).

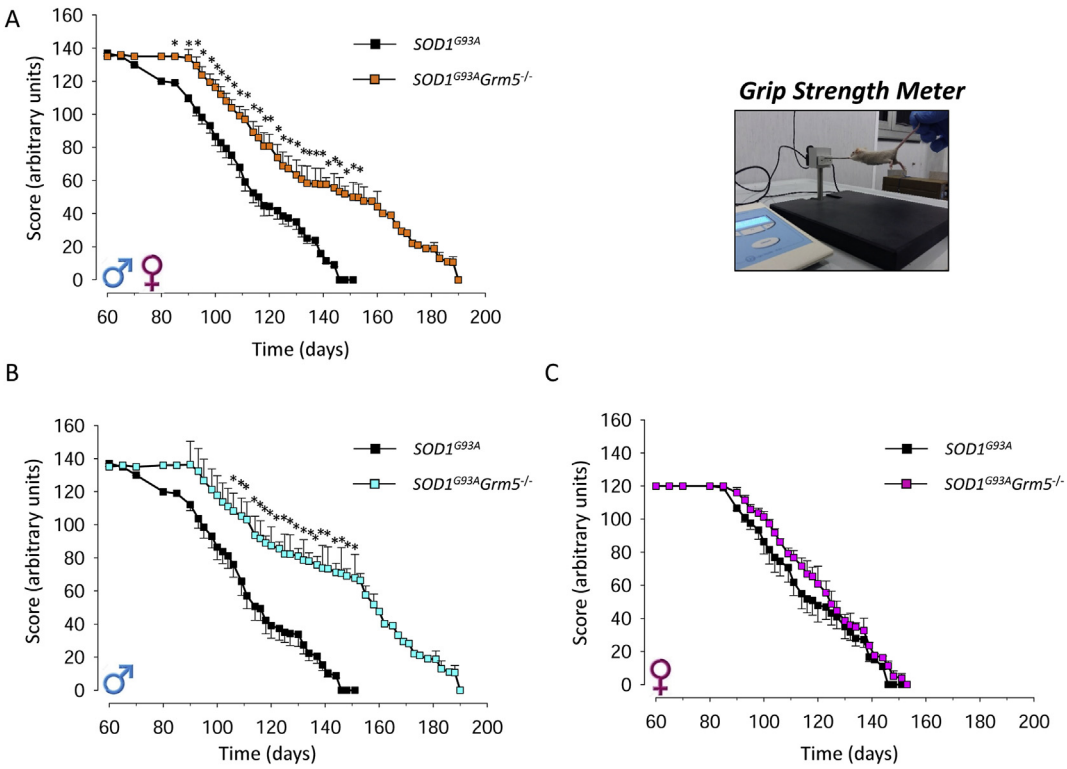

Fig. 10. Grip strength meter test in $SOD1^{G93A}$ and $SOD1^{G93A}Grm5^{-/-}$ mice. The Grip strength meter test was used to determine fore limb muscle strength differences during the disease progression between $SOD1^{G93A}$ and $SOD1^{G93A}Grm5^{-/-}$ in male + female (A), male (B), and female (C) mice. Animals were tested 3 days a week starting on day 90. Animals were allowed to grasp the pull bar of a motor-aided dynamometer and the maximal fore limb force was recorded. Data are means ± s.e.m. of 12 $SOD1^{G93A}$ and 9 $SOD1^{G93A}Grm5^{-/-}$ males and of 12 $SOD1^{G93A}$ and 7 $SOD1^{G93A}Grm5^{-/-}$ females. $^{*}p < .05$ at least (one-tail Student *t*-test).

Nakao et al., 2007). To note, ablation of mGluR5 ameliorated motor coordination also in ataxic $Grm1^{crv4/crv4}$ mice (Bossi et al., 2018). Therefore, we focused our attention on the $SOD1^{G93A}Grm5^{-/-}$ double mutant, knockout for mGluR5, that did not show any evident phenotypic alteration. As a matter of facts, $Grm5^{-/-}$ mouse phenotype has been mainly associated with cognitive deficits, such as impaired spatial learning and reduced long-term potentiation in the hippocampal CA1-dentate gyrus pathway (Lu et al., 1997). The main in-vivo aspect linked to the mGluR5 ablation is represented by schizophrenia-related behavioural changes, including deficit of pre-pulse inhibition to a startling stimulus (Brody et al., 2004; Luoni et al., 2018). Related to motor function, it has been recently demonstrated that $Grm5^{-/-}$ mice show a normal sensorimotor gating as well as no impairment in motor balance/learning (Jew et al., 2013), thus avoiding possible erroneous interpretation of data in the present work.

Abolishing mGluR5 in $SOD1^{G93A}$ mice overall led to a pronounced improvement of the ALS clinical scores related to disease onset, survival and to the comprehensive battery of behavioural tasks analyzed during the disease course, as well as preservation of spinal cord MNs and normalization of the astrocyte and microglia reactive phenotype. Relevant improvements obtained here in $SOD1^{G93A}Grm5^{-/-}$ mice, respect to $SOD1^{G93A}Grm5^{-/+}$ mice (Bonifacino et al., 2017), are (i) a substantial survival extension in male mice; (ii) a remarkable increase in Rotarod, extension reflex, and gait performances in male mice; (iii) most relevant, amelioration of motor skills in female $SOD1^{G93A}Grm5^{-/-}$ mice, that were not observed in the previous study in $SOD1^{G93A}Grm5^{-/+}$ mice. Although the amelioration of symptoms in female $SOD1^{G93A}Grm5^{-/-}$ mice was still less pronounced than in males, the observed improvements were always significant, except for the Grip strength meter test.

The reason for the presence of motor skill gender differences is not obvious. One possible cause could rely on the gender differences

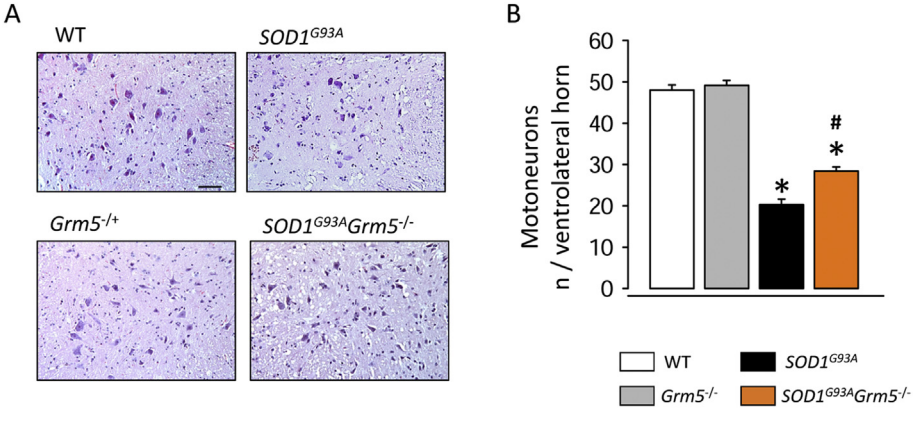

Fig. 11. Motor neuron count in spinal cord of WT, $Grm5^{-/-}$, $SOD1^{G93A}$, and $SOD1^{G93A}Grm5^{-/-}$ mice. The number of MNs has been assessed in lumbar spinal cord sections of 110 day-old mice after staining with haematoxylin and eosin. MNs were selected and counted based on diameters > 25 µm. Representative photomicrographs of lumbar spinal cord sections (A; scale bar 100 µm) and quantitative analysis (B) are reported. Data are means ± s.e.m. of 3 independent experiments (3 mice per group, 6/7 sections per mouse; WT mice: 1 male and 2 females; $Grm5^{-/-}$ mice: 1 male and 2 female; $SOD1^{G93A}$ mice: 1 male and 2 females; $SOD1^{G93A}Grm5^{-/-}$ mice: 1 male and 2 female). $^{*}p < .001$ vs. the respective control; $^{\#}p < .01$ vs. $SOD1^{G93A}$ mice (One-way ANOVA followed by Bonferroni post-hoc tests).

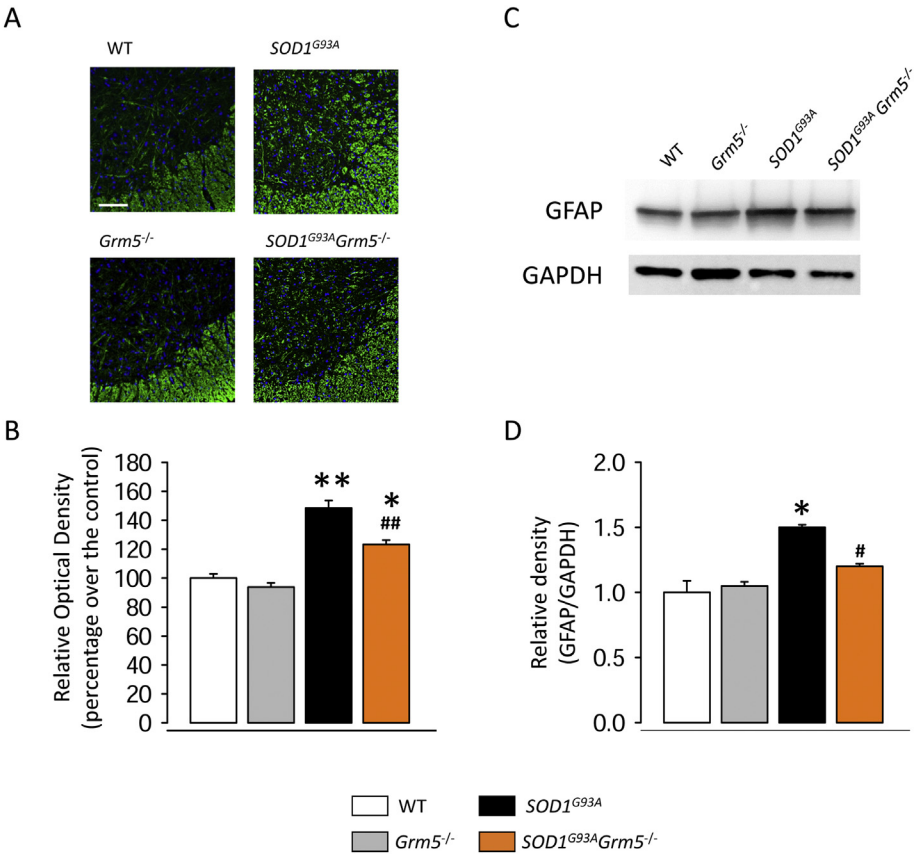

Fig. 12. Astrogliosis in spinal cord from of WT, *Grm5*$^{-/-}$, *SOD1*^{G93A}, and *SOD1*^{G93A}*Grm5*$^{-/-}$ mice. The expression of GFAP was measured as an index of astrogliosis. GFAP was determined in lumbar spinal cord slices by immunofluorescence (IF) and confocal microscopy and in homogenates by SDS-PAGE and WB using a mouse anti-GFAP monoclonal antibody. IF representative images (A, scale bar 200 μm), IF quantitative analysis (B), WB representative immunoreactive bands (C), and WB quantitative analysis (D) are reported. Confocal microscopy data are means ± s.e.m. of 3 independent experiments in triplicate (3 mice per group; 3 section per mouse; WT mice: 1 male and 2 females; *Grm5*$^{-/-}$ mice: 2 males and 1 female; *SOD1*^{G93A} mice: 1 male and 2 females; *SOD1*^{G93A}*Grm5*$^{-/-}$ mice: 1 male and 2 females). WB data are means ± s.e.m. of 3 independent experiments in triplicate (3 mice per group, 3 loading per mouse; WT mice: 2 males and 1 female; *Grm5*$^{-/-}$ mice: 1 male and 2 females; *SOD1*^{G93A} mice: 2 males and 1 female; *SOD1*^{G93A}*Grm5*$^{-/-}$ mice: 2 males and 1 female). $^{*}p < .01$ and $^{**}p < .001$ vs. the respective control; $^{\#}p < .05$ and $^{\#\#}p < .001$ vs. *SOD1*^{G93A} mice (One-way ANOVA followed by Bonferroni's post-hoc tests).

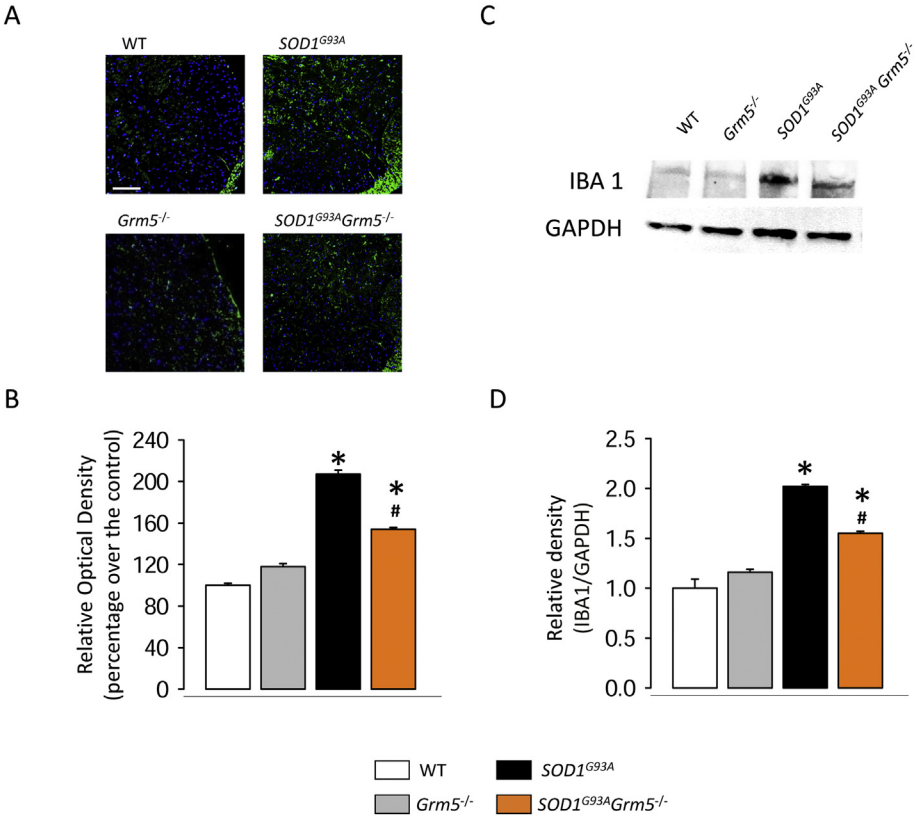

Fig. 13. Microgliosis in spinal cord from WT, *Grm5*$^{-/-}$, *SOD1*^{G93A}, and *SOD1*^{G93A}*Grm5*$^{-/-}$ mice. The expression of IBA-1 was measured as an index of microgliosis. IBA-1 was determined in lumbar spinal cord slices by immunofluorescence (IF) and confocal microscopy and in homogenates by SDS-PAGE and WB, using a goat anti-IBA-1 polyclonal antibody. Representative IF images (A, scale bar 200 μm), IF quantitative analysis (B), representative WB immunoreactive bands (C), and WB quantitative analysis (D) are reported. Confocal microscopy data are means ± s.e.m. of 3 independent experiments in triplicate (3 mice per group; 3 sections per mouse; WT mice: 1 male and 2 females; *Grm5*$^{-/-}$ mice: 2 males and 1 female; *SOD1*^{G93A} mice: 1 male and 2 females; *SOD1*^{G93A}*Grm5*$^{-/-}$ mice: 1 male and 2 female). WB data are means ± s.e.m. of 3 independent experiments in triplicate (3 mice per group, 3 loading per mouse; WT mice: 2 males and 1 female; *Grm5*$^{-/-}$ mice: 1 male and 2 females; *SOD1*^{G93A} mice: 2 males and 1 female; *SOD1*^{G93A}*Grm5*$^{-/-}$ mice: 2 males and 1 female). $^{*}p < .001$ vs. the respective controls; $^{\#}p < .001$ vs. *SOD1*^{G93A} (One-way ANOVA followed by Bonferroni's post-hoc tests).

already present in *SOD1*^{G93A} mice. It is well known that *SOD1*^{G93A} females show higher survival probability and motor ability than *SOD1*^{G93A} males. This improved starting point could have led to underestimate the positive effect of reducing mGluR5 expression. The difference might base on the mixed B6SJL genetic background of *SOD1*^{G93A} mice. The background-dependent gender differences are indeed confirmed by numerous studies (see Pfohl et al., 2015 for a meta-analysis on 97 studies). We crossed here mice carrying dissimilar genetic background (C57BL6-B6SJL *SOD1*^{G93A} mice and B6.129 *Grm5*$^{+/-}$ mice) to reduce the expression of mGluR5 and this procedure could have further adapted the gender response. It should be also considered that halving mGluR1 expression also led to reduction of mGluR5 (Milanese et al., 2014), while reducing mGluR5 expression did not modify mGluR1 (Bonifacino et al., 2017 and present results). The existence of mGlu1R/mGluR5 heterodimers has been directly demonstrated (Doumazane et al., 2011; Pandya et al., 2016), thus altering the expression of mGluR5, but not of mGluR1 (Bonifacino et al., 2017; Fig. 1), could change the association of mGluR1/mGluR5 heterodimers, possibly modifying some of the pathological traits, with different gender impact.

As to the possible contribution of MN survival to gender differences in motor function, the data collected do not allow to elucidate this issue at present since no apparent differences could be detected. The same was true for the amelioration of astrocyte and microglia phenotype. A more in-dept analysis is worthy to be undertaken in future studies. We showed here that the massive loss of MNs in the ventral horns of the lumbar spinal cord, a typical hallmark of ALS end-stage, was partially improved after deleting mGluR5 in the *SOD1*^{G93A} background. This observation is particularly remarkable considering that the analyses have been performed in mice at an advanced stage of the disease. Damage of MNs in ALS is a non-cell autonomous event (Ilieva et al., 2009; Lee et al., 2016) and astrocytes retain a pivotal role in affecting disease progression (Yamanaka et al., 2008; Wang et al., 2011) and MN vulnerability to excitotoxicity (Van Damme et al., 2007). Moreover, reducing mutated SOD1 expression in microglia also produced beneficial effects on disease duration and extended survival in *SOD1*^{G93A} mice (Beers et al., 2006; Boillée et al., 2006). We observed here a reduction in astrogliosis and microgliosis in *SOD1*^{G93A}*Grm5*$^{-/-}$ mice, assessed by monitoring GFAP and IBA-1 expression, which possibly ameliorates the noxious milieu surrounding MNs, protecting MNs from death and reducing the disease severity.

Due to the multifactorial features of ALS (Andersen and Al-Chalabi, 2011) and to the well-recognized non-cellular autonomous characteristics of the disease (Ilieva et al., 2009; Lee et al., 2016), each patient likely represents a unique clinical case that should be treated by targeting the appropriate etiological causes. Accordingly, it is a current belief that a successful therapy should be multimodal. Targeting Glu transmission in ALS operating at mGluR1 and mGluR5 may have the advantage of modifying an up-stream phenomenon which in turn affect many down-stream pathways, mimicking a multi-approach therapy.

In conclusion, the present and previous results obtained by constitutively reducing mGluR5 expression in *SOD1*^{G93A} mice emphasize the role of these receptors in ALS, the hyperactivity of which could represent a central mechanism contributing to the disease progression. This genetically-based evidence points to the importance of verifying whether pharmacological treatments with mGluR5 antagonists can be effective in counteracting ALS.

Declaration of competing interests

The authors have no conflict of interest.

Funding

This work was supported by grants from the Italian Ministry of Education, University and Research (SIR project n.RBSI14B1Z1 to MM and PRIN project No. 2016058401 to GB) and from the Motor Neurone Disease Association (Project No. April16/848-791 to GB). SB is supported by the grant “Fondi Ricerca Ateneo (FRA)” from the University of Genoa.

Acknowledgements

The authors gratefully acknowledge the undergraduate student Marta Oliveri for her helpful technical support.

References

Alfieri, J.A., Pino, N.S., Igaz, L.M., 2014. Reversible behavioral phenotypes in a conditional mouse model of tdp-43 proteinopathies. J. Neurosci. 34 (46), 15244–15259. https://doi.org/10.1523/JNEUROSCI.1918-14.2014.

Alsultan, A.A., Waller, R., Heath, P.R., Kirby, J., 2016. The genetics of amyotrophic lateral sclerosis: current insights. Degener. Neurol. Neuromuscul. Dis. 6, 49–64. https://doi.org/10.2147/DNND.S84956.

Andersen, P.M., Al-Chalabi, A., 2011. Clinical genetics of amyotrophic lateral sclerosis: what do we really know? Nat. Rev. Neurol. 7 (11), 603–615. https://doi.org/10.1038/nrneurol.2011.150.

Anneser, J.M., Borasio, G.D., Berthele, A., Zieglgänsberger, W., Tölle, T.R., 1999. Differential expression of group I metabotropic glutamate receptors in rat spinal cord somatic and autonomic motoneurons: possible implications for the pathogenesis of amyotrophic lateral sclerosis. Neurobiol. Dis. 6 (2), 140–147. https://doi.org/10.1006/nbdi.1999.0237.

Anneser, J.M., Ince, P.G., Shaw, P.J., Borasio, G.D., 2004. Differential expression of mGluR5 in human lumbosacral motoneurons. Neuroreport. 15 (2), 271–273. https://doi.org/10.1097/01.wnr.0000109796.20952.eb.

Aronica, E., Catania, M.V., Geurts, J., Yankaya, B., Troost, D., 2001. Immunohistochemical localization of group I and II metabotropic glutamate receptors in control and amyotrophic lateral sclerosis human spinal cord: upregulation in reactive astrocytes. Neuroscience 105 (2), 509–520. https://doi.org/10.1016/S0306-4522(01)00181-6.

Battaglia, G., Bruno, V., 2018. Metabotropic glutamate receptor involvement in the pathophysiology of amyotrophic lateral sclerosis: new potential drug targets for therapeutic applications. Curr. Opin. Pharmacol. 38, 65–71. https://doi.org/10.1016/j.coph.2018.02.007.

Beers, D.R., Henkel, J.S., Xiao, Q., Zhao, W., Wang, J., Yen, A.A., Siklos, L., McKercher, S.R., Appel, S.H., 2006. Wild-type microglia extend survival in PU.1 knockout mice with familial amyotrophic lateral sclerosis. Proc. Natl. Acad. Sci. U. S. A. 103 (43), 16021–16026. https://doi.org/10.1073/pnas.0607423103.

Boillée, S., Yamanaka, K., Lobsiger, C.S., Copeland, N.G., Jenkins, N.A., Kassiotis, G., Kollias, G., Cleveland, D.W., 2006. Onset and progression in inherited ALS determined by motor neurons and microglia. Science. 312 (5778), 1389–1392. https://doi.org/10.1126/science.1123511\.

Bonifacino, T., Musazzi, L., Milanese, M., Seguini, M., Marte, A., Gallia, E., Cattaneo, L., Onofri, F., Popoli, M., Bonanno, G., 2016. Altered mechanisms underlying the abnormal glutamate release in amyotrophic lateral sclerosis at a pre-symptomatic stage of the disease. Neurobiol. Dis. 95, 122–133. https://doi.org/10.1016/j.nbd.2016.07.011.

Bonifacino, T., Cattaneo, L., Gallia, E., Puliti, A., Melone, M., Provenzano, F., Bossi, S., Musante, I., Usai, C., Conti, F., Bonanno, G., Milanese, M., 2017. In-vivo effects of knocking-down metabotropic glutamate receptor 5 in the SOD1G93A mouse model of amyotrophic lateral sclerosis. Neuropharmacology. 123, 433–445. https://doi.org/10.1016/j.neuropharm.2017.06.020.

Bossi, S., Musante, I., Bonfiglio, T., Bonifacino, T., Emionite, L., Cerminara, M., Cervetto, C., Marcoli, M., Bonanno, G., Ravazzolo, R., Pittaluga, A., Puliti, A., 2018. Genetic inactivation of mGlu5 receptor improves motor coordination in the Grm1crv4 mouse model of SCAR13 ataxia. Neurobiol. Dis. 109, 44–53. https://doi.org/10.1016/j.nbd.2017.10.001. Pt A.

Bradford, M.M., 1976. A rapid and sensitive method for the quantitation of microgram quantities of protein utilizing the principle of protein-dyebinding. Anal. Biochem. 72, 248–254. https://doi.org/10.1016/0003-2697(76)90527-3.

Brody, S.A., Dulawa, S.C., Conquet, F., Geyer, M.A., 2004. Assessment of a prepulse inhibition deficit in a mutant mouse lacking mglu5 receptors. Mol. Psychiatry 9, 35–41. https://doi.org/10.1038/sj.mp.4001404.

Cardiff, R.D., Miller, C.H., Munn, R.J., 2014. Manual hematoxylin and eosin staining of mouse tissue sections. Cold Spring Harb Protoc 2014 (6), 655–658. https://doi.org/10.1101/pdb.prot073411.

Cleveland, D.W., Rothstein, J.D., 2001. From Charcot to Lou Gehrig: deciphering selective motor neuron death in ALS. Nat. Rev. Neurosci. 2 (11), 806–819. https://doi.org/10.1038/35097565.

Cleveland, D.W., Bruijn, L.I., Wong, P.C., Marszalek, J.R., Vechio, J.D., Lee, M.K., Xu, X.S., Borchelt, D.R., Sisodia, S.S., Price, D.L., 1996. Mechanisms of selective motor neuron death in transgenic mouse models of motor neuron disease. Neurology. 47 (4 Suppl 2), S54–S61 (discussion S61–62. Review).

Conti, F., Weinberg, R.J., 1999. Shaping excitation at glutamatergic synapses. Trends Neurosci. 22 (10), 451–458. https://doi.org/10.1016/S0166-2236(99)01445-9.

Conti, V., Aghaie, A., Cilli, M., Martin, N., Caridi, G., Musante, L., Candiano, G., Castagna, M., Fairen, A., Ravazzolo, R., Guenet, J.L., Puliti, A., 2006. crv4, a mouse model for human ataxia associated with kyphoscoliosis caused by an mRNA splicing mutation

of the metabotropic glutamate receptor 1 (Grm1). Int. J. Mol. Med. 18 (4), 593–600. https://doi.org/10.3892/ijmm.18.4.593.
D'Antoni, S., Berretta, A., Seminara, G., Longone, P., Giuffrida-Stella, A.M., Battaglia, G., Sortino, M.A., Nicoletti, F., Catania, M.V., 2011. A prolonged pharmacological blockade of type-5 metabotropic glutamate receptors protects cultured spinal cord motor neurons against excitotoxic death. Neurobiol. Dis. 42 (3), 252–264. https://doi.org/10.1016/j.nbd.2011.01.013.
Degos, V., Peineau, S., Nijboer, C., Kaindl, A.M., Sigaut, S., Favrais, G., Plaisant, F., Teissier, N., Gouadon, E., Lombet, A., Saliba, E., Collingridge, G.L., Maze, M., Nicoletti, F., Heijnen, C., Mantz, J., Kavelaars, A., Gressens, P., 2013. G protein-coupled receptor kinase 2 and group I metabotropic glutamate receptors mediate inflammation-induced sensitization to excitotoxic neurodegeneration. Ann. Neurol. 73 (5), 667–678. https://doi.org/10.1002/ana.23868.
Dingledine, R., Borges, K., Bowie, D., Traynelis, S.F., 1999. The glutamate receptor ion channels. Pharmacol. Rev. 51 (1), 7–61 (Review).
Doumazane, E., Scholler, P., Zwier, J.M., Trinquet, E., Rondard, P., Pin, J.P., 2011. A new approach to analyze cell surface protein complexes reveals specific heterodimeric metabotropic glutamate receptors. FASEB J. 25 (1), 66–77. https://doi.org/10.1096/fj.10-163147.
Eisen, A., 2009. Amyotrophic lateral sclerosis – evolutionary and other perspectives. Muscle Nerve 40 (2), 297–304. https://doi.org/10.1002/mus.21404.
Ferraiuolo, L., Kirby, J., Grierson, A.J., Sendtner, M., Shaw, P.J., 2011. Molecular pathways of motorneuron injury in amyotrophic lateral sclerosis. Nat. Rev. Neurol. 7 (11), 616–630. https://doi.org/10.1038/nrneurol.2011.152.
Giribaldi, F., Milanese, M., Bonifacino, T., Rossi, P.I.A., Di Prisco, S., Pittaluga, A., Tacchetti, C., Puliti, A., Usai, C., Bonanno, G., 2013. Group I metabotropic glutamate autoreceptors induce abnormal glutamate exocytosis in a mouse model of amyotrophic lateral sclerosis. Neuropharmacology. 66, 253–263. https://doi.org/10.1016/j.neuropharm.2012.05.018.
Gurney, M.E., Pu, H., Chiu, A.Y., Dal Canto, M.C., Polchow, C.Y., Alexander, D.D., Caliendo, J., Hentati, A., Kwon, Y.W., Deng, H.X., et al., 1994. Motor neuron degeneration in mice that express a human Cu, Zn superoxide dismutase mutation. Science. 264 (5166), 1772–1775 (Erratum in: Science 10.1126/science.8209258).
Ilieva, H., Polymenidou, M., Cleveland, D.W., 2009. Non-cell autonomous toxicity in neurodegenerative disorders: ALS and beyond. J. Cell Biol. 187 (6), 761–772. https://doi.org/10.1083/jcb.200908164.
Jew, C.P., Wu, C.S., Sun, H., Zhu, J., Huang, J.Y., Yu, D., Justice, N.J., Lu, H.C., 2013. MGluR5 ablation in cortical glutamatergic neurons increases novelty-induced locomotion. PLoS One 8 (8), e70415. https://doi.org/10.1371/journal.pone.0070415.
King, A.E., Woodhouse, A., Kirkcaldie, M.T., Vickers, J.C., 2016. Excitotoxicity in ALS: overstimulation, or overreaction? Exp. Neurol. 1, 162–171. 275 Pt. Review. https://doi.org/10.1016/j.expneurol.2015.09.019.
Kuner, R., Groom, A.J., Müller, G., Kornau, H.C., Stefovska, V., Bresink, I., Hartmann, B., Tschauner, K., Waibel, S., Ludolph, A.C., Ikonomidou, C., Seeburg, P.H., Turski, L., 2005. Mechanisms of disease: motoneuron disease aggravated by transgenic expression of a functionally modified AMPA receptor subunit. Ann. N. Y. Acad. Sci. 1053, 269–286. https://doi.org/10.1196/annals.1344.024.
Laferriere, F., Polymenidou, M., 2015. Advances and challenges in understanding the multifaceted pathogenesis of amyotrophic lateral sclerosis. Swiss Med. Wkly. 145, w14054. https://doi.org/10.4414/smw.2015.14054.
Lasiene, J., Yamanaka, K., 2011. Glial cells in amyotrophic lateral sclerosis. Neurol. Res. Int. 2011, 718987. https://doi.org/10.1155/2011/718987.
Lazarevic, V., Yang, Y., Ivanova, D., Fejtova, A., Svenningsson, P., 2018. Riluzole attenuates the efficacy of glutamatergic transmission by interfering with the size of the readily releasable neurotransmitter pool. Neuropharmacology 143, 38–48. https://doi.org/10.1016/j.neuropharm.2018.09.021.
Lee, J., Hyeon, S.J., Im, H., Ryu, H., Kim, Y., Ryu, H., 2016. Astrocytes and microglia as non-cell autonomous players in the pathogenesis of ALS. Exp. Neurobiol. 25 (5), 233–240. https://doi.org/10.5607/en.2016.25.5.233.
Lu, Y.M., Jia, Z., Janus, C., Henderson, J.T., Gerlai, R., Wojtowicz, J.M., Roder, J.C., 1997. Mice lacking metabotropic glutamate receptor 5 show impaired learning and reduced CA1 long-termpotentiation (LTP) butnormal CA3 LTP. J. Neurosci. 17 (13), 5196–5205. https://doi.org/10.1523/JNEUROSCI.17-13-05196.1997.
Luong, T.N., Carlisle, H.J., Southwell, A., Patterson, P.H., 2011. Assessment of motor balance and coordination in mice using the balance beam. J. Vis. Exp. 10 (49). https://doi.org/10.3791/2376. pii: 2376.
Luoni, A., Gass, P., Brambilla, P., Ruggeri, M., Riva, M.A., Inta, D., 2018. Altered expression of schizophrenia-related genes in mice lacking mglu5 receptors. Eur. Arch. Psychiatry Clin. Neurosci. 268 (1), 77–87. https://doi.org/10.1007/s00406-016-0728-z.
Martorana, F., Brambilla, L., Valori, C.F., Bergamaschi, C., Roncoroni, C., Aronica, E., Volterra, A., Bezzi, P., Rossi, D., 2012. The BH4 domain of Bcl-X(L) rescues astrocyte degeneration in amyotrophic lateral sclerosis by modulating intracellular calcium signals. Hum. Mol. Genet. 21 (4), 826–840. https://doi.org/10.1093/hmg/ddr513.
Milanese, M., Zappettini, S., Jacchetti, E., Bonifacino, T., Cervetto, C., Usai, C., Bonanno, G., 2010. In-vitro activation of GAT1 transporters expressed in spinal cord gliosomes stimulates glutamate release that is abnormally elevated in the SOD1/G93A(+) mouse model of amyotrophic lateral sclerosis. J. Neurochem. 113, 489–501. https://doi.org/10.1111/j.1471-4159.2010.06628.x.
Milanese, M., Zappettini, S., Onofri, F., Musazzi, L., Tardito, D., Bonifacino, T., Messa, M., Racagni, G., Usai, C., Benfenati, F., Popoli, M., Bonanno, G., 2011. Abnormal exocytotic release of glutamate in a mouse model of amyotrophic lateral sclerosis. J. Neurochem. 116 (6), 1028–1042. https://doi.org/10.1111/j.1471-4159.2010.07155.x.
Milanese, M., Giribaldi, F., Melone, M., Bonifacino, T., Musante, I., Carminati, E., Rossi, P.I., Vergani, L., Voci, A., Conti, F., Puliti, A., Bonanno, G., 2014. Knocking down metabotropic glutamate receptor 1 improves survival and disease progression in the SOD1(G93A) mouse model of amyotrophic lateral sclerosis. Neurobiol. Dis. 64, 48–59. https://doi.org/10.1016/j.nbd.2013.11.006.
Milanese, M., Bonifacino, T., Fedele, E., Rebosio, C., Cattaneo, L., Benfenati, F., Usai, C., Bonanno, G., 2015. Exocytosis regulates trafficking of GABA and glycine heterotransporters in spinal cord glutamatergic synapses: a mechanism for the excessive heterotransporter-induced release of glutamate in experimental amyotrophic lateral sclerosis. Neurobiol. Dis. 74, 314–324. https://doi.org/10.1016/j.nbd.2014.12.004.
Morrison, B.M., Morrison, J.H., 1999. Amyotrophic lateral sclerosis associated with mutations in superoxide dismutase: a putative mechanism of degeneration. Brain Res. Rev. 29 (1), 121–135. Review. https://doi.org/10.1016/S0165-0173(98)00049-6.
Musante, V., Neri, E., Feligioni, M., Puliti, A., Pedrazzi, M., Conti, V., Usai, C., Diaspro, A., Ravazzolo, R., Henley, J.M., Battaglia, G., Pittaluga, A., 2008. Presynaptic mGlu1 and mGlu5 autoreceptors facilitate glutamate exocytosis from mouse cortical nerve endings. Neuropharmacology. 55 (4), 474–482. https://doi.org/10.1016/j.neuropharm.2008.06.056.
Nakao, H., Nakao, K., Kano, M., Aiba, A., 2007. Metabotropic glutamate receptor subtype-1 is essential for motor coordination in the adult cerebellum. Neurosci. Res. 57 (4), 538–543. https://doi.org/10.1016/j.neures.2006.12.014.
Nicoletti, F., Bockaert, J., Collingridge, G.L., Conn, P.J., Ferraguti, F., Schoepp, D.D., Wroblewski, J.T., Pin, J.P., 2011. Metabotropic glutamate receptors: from the workbench to the bedside. Neuropharmacology. 60 (7–8), 1017–1041. Review. https://doi.org/10.1016/j.neuropharm.2010.10.022.
Pandya, N.J., Klaassen, R.V., van der Schors, R.C., Slotman, J.A., Houtsmuller, A., Smit, A.B., Li, K.W., 2016. Group I metabotropic glutamate receptors 1 and 5 form a protein complex in mouse hippocampus and cortex. Proteomics. 16 (20), 2698–2705. https://doi.org/10.1002/pmic.201500400.
Perry, T.L., Krieger, C., Hansen, S., Eisen, A., 1990. Amyotrophic lateral sclerosis: amino acid levels in plasma and cerebro spinal fluid. Ann. Neurol. 28 (1), 12–17. https://doi.org/10.1002/ana.410280105.
Peters, O.M., Ghasemi, M., Brown Jr., R.H., 2015. Emerging mechanisms of molecular pathology in ALS. J. Clin. Invest. 125 (6), 2548. https://doi.org/10.1172/JCI71601.
Pfohl, S.R., Halicek, M.T., Mitchell, C.S., 2015. Characterization of the contribution of genetic background and gender to disease progression in the SOD1G93A mouse model of amyotrophic lateral sclerosis: a meta-analysis. J. Neuromuscul. Dis. 2 (2), 137–150. https://doi.org/10.3233/JND-140068.
Pin, J.P., Acher, F., 2002. The metabotropic glutamate receptors: structure, activation mechanism and pharmacology. Curr. Drug Targets CNS Neurol. Disord. 1 (3), 297–317. Review. https://doi.org/10.2174/1568007023339328.
Pin, J.P., Duvoisin, R., 1995. The metabotropic glutamate receptors: structure and functions. Neuropharmacology. 34 (1), 1–26. https://doi.org/10.1016/0028-3908(94)00129-G.
Pittaluga, A., 2016. Presynaptic release-regulating mGlu1 receptors in central nervous system. Front. Pharmacol. 7, 295. Review. https://doi.org/10.3389/fphar.2016.00295.
Raiteri, L., Paolucci, E., Prisco, S., Raiteri, M., Bonanno, G., 2003. Activation of a glycine transporter on spinal cord neurons causes enhanced glutamate release in a mouse model of amyotrophic lateral sclerosis. Br. J. Pharmacol. 138 (6), 1021–1025. https://doi.org/10.1038/sj.bjp.0705142.
Raiteri, L., Stigliani, S., Zappettini, S., Mercuri, N.B., Raiteri, M., Bonanno, G., 2004. Excessive and precocious glutamate release in a mouse model of amyotrophic lateral sclerosis. Neuropharmacology. 46 (6), 782–792. https://doi.org/10.1016/j.neuropharm.2003.11.025.
Ravera, S., Bartolucci, M., Adriano, E., Garbati, P., Ferrando, S., Ramoino, P., Calzia, D., Morelli, A., Balestrino, M., Panfoli, I., 2016. Support of nerve conduction by respiring myelin sheath: role of connexons. Mol. Neurobiol. 53, 2468–2479. https://doi.org/10.1007/s12035-015-9216-0.
Rossi, D., Brambilla, L., Valori, C.F., Roncoroni, C., Crugnola, A., Yokota, T., Bredesen, D.E., Volterra, A., 2008. Focal degeneration of astrocytes in amyotrophic lateral sclerosis. Cell Death Differ. 15 (11), 1691–1700. https://doi.org/10.1038/cdd.2008.99.
Rossi, P.I., Musante, I., Summa, M., Pittaluga, A., Emionite, L., Ikehata, M., Rastaldi, M.P., Ravazzolo, R., Puliti, A., 2013. Compensatory molecular and functional mechanisms in nervous system of the grm1(crv4) mouse lacking the mGlu1 receptor: a model for motor coordination deficits. Cereb. Cortex 23, 2179–2189. https://doi.org/10.1093/cercor/bhs200.
Rothstein, J.D., Tsai, G., Kuncl, R.W., Clawson, L., Cornblath, D.R., Drachman, D.B., Pestronk, A., Stauch, B.L., Coyle, J.T., 1990. Abnormal excitatory amino acid metabolism in amyotrophic lateral sclerosis. Ann. Neurol. 28 (1), 18–25. https://doi.org/10.1002/ana.410280106.
Rothstein, J.D., Van Kammen, M., Levey, A.I., Martin, L.J., Kuncl, R.W., 1995. Selective loss of glial glutamate transporter GLT-1 in amyotrophic lateral sclerosis. Ann. Neurol. 38 (1), 73–84. https://doi.org/10.1002/ana.410380114.
Seo, J.S., Baek, I.S., Leem, Y.H., Kim, T.K., Cho, Y., Lee, S.M., Park, Y.H., Han, P.L., 2011. SK-PC-B70M alleviates neurologic symptoms in G93A-SOD1 amyotrophic lateral sclerosis mice. Brain Res. 1368, 299–307. https://doi.org/10.1016/j.brainres.2010.10.048.
Shaw, P.J., Eggett, C.J., 2000. Molecular factors underlying selective vulnerability of motor neurons to neurodegeneration in amyotrophic lateral sclerosis. J. Neurol. 247 (Suppl. 1), I17–I27. Review. https://doi.org/10.1007/BF03161151.
Shaw, P.J., Forrest, V., Ince, P.G., Richardson, J.P., Wastell, H.J., 1995. CSF and plasma amino acid levels in motorneuron disease: elevation of CSF glutamate in a subset of patients. Neurodegeneration. 4 (2), 209–216. https://doi.org/10.1006/neur.1995.0026.
Spreux-Varoquaux, O., Bensimon, G., Lacomblez, L., Salachas, F., Pradat, P.F., Le Forestier, N., Marouan, A., Dib, M., Meininger, V., 2002. Glutamate levels in cerebro

spinal fluid in amyotrophic lateral sclerosis: a reappraisal using a new HPLC method with coulometric detection in a large cohort of patients. J. Neurol. Sci. 193 (2), 73–78. https://doi.org/10.1016/S0022-510X(01)00661-X.

Stifanese, R., Averna, M., De Tullio, R., Pedrazzi, M., Beccaria, F., Salamino, F., Milanese, M., Bonanno, G., Pontremoli, S., Melloni, E., 2010. Adaptive modifications in the calpain/calpastatin system in brain cells after persistent alteration in Ca2+ homeostasis. J. Biol. Chem. 285 (1), 631–643. https://doi.org/10.1074/jbc.M109.031674.

Swanson, C.J., Kalivas, P.W., 2000. Regulation of locomotor activity by metabotropic glutamate receptors in the nucleus accumbens and ventral tegmental area. J. Pharmacol. Exp. Ther. 292 (1), 406–414.

Tan, W., Pasinelli, P., Trotti, D., 2014. Role of mitochondria in mutant SOD1 linked amyotrophic lateral sclerosis. Biochim. Biophys. Acta 1842 (8), 1295–1301. Review. https://doi.org/10.1016/j.bbadis.2014.02.009.

Tortarolo, M., Grignaschi, G., Calvaresi, N., Zennaro, E., Spaltro, G., Colovic, M., Fracasso, C., Guiso, G., Elger, B., Schneider, H., Seilheimer, B., Caccia, S., Bendotti, C., 2006. Glutamate AMPA receptors change in motor neurons of SOD1G93A transgenic mice and their inhibition by a non competitive antagonist ameliorates the progression of amyotrophic lateral sclerosis-like disease. J. Neurosci. Res. 83 (1), 134–146. https://doi.org/10.1002/jnr.20715.

Uccelli, A., Milanese, M., Principato, M.C., Morando, S., Bonifacino, T., Vergani, L., Giunti, D., Voci, A., Carminati, E., Giribaldi, F., Caponnetto, C., Bonanno, G., 2012. Intravenous mesenchymal stem cells improve survival and motor function in experimental amyotrophic lateral sclerosis. Mol. Med. 18, 794–804. https://doi.org/10.2119/molmed.2011.00498.

Valerio, A., Ferrario, M., Paterlini, M., Liberini, P., Moretto, G., Cairns, N.J., Pizzi, M., Spano, P., 2002. Spinal cord mGlu1a receptors: possible target for amyotrophic lateral sclerosis therapy. Pharmacol. Biochem. Behav. 73 (2), 447–454. https://doi.org/10.1016/S0091-3057(02)00835-3.

Van Damme, P., Bogaert, E., Dewi,l, M., Hersmus, N., Kiraly, D., Scheveneels, W., Bockx, I., Braeken, D., Verpoorten, N., Verhoeven, K., Timmerman, V., Herijgers, P., Callewaert, G., Carmeliet, P., Van Den Bosch, L., Robberecht, W., 2007. Astrocytes regulate GluR2 expression in motor neurons and their vulnerability to excitotoxicity. Proc. Natl. Acad. Sci. U. S. A. 104 (37), 14825–14830. https://doi.org/10.1073/pnas.0705046104.

Van Den Bosch, L., Vandenberghe, W., Klaassen, H., Van Houtte, E., Robberecht, W., 2000. Ca(2+)-permeable AMPA receptors and selective vulnerability of motor neurons. J. Neurol. Sci. 180 (1–2), 29–34. https://doi.org/10.1016/S0022-510X(00)00414-7.

Van Den Bosch, L., Van Damme, P., Bogaert, E., Robberecht, W., 2006. The role of excitotoxicity in the pathogenesis of amyotrophic lateral sclerosis. Biochim. Biophys. Acta 1762 (11−12), 1068–1082. Review. https://doi.org/10.1016/j.bbadis.2006.05.002.

Wang, L., Gutmann, D.H., Roos, R.P., 2011. Astrocyte loss of mutant SOD1 delays ALS disease onset and progression in G85R transgenic mice. Hum. Mol. Genet. 20 (2), 286–293. https://doi.org/10.1093/hmg/ddq463.

Wuolikainen, A., Moritz, T., Marklund, S.L., Antti, H., Andersen, P.M., 2011. Disease-related changes in the cerebro spinal fluid metabolome in amyotrophic lateral sclerosis detected by GC/TOFMS. PLoS One 6 (4), e17947. https://doi.org/10.1371/journal.pone.0017947.

Yamanaka, K., Chun, S.J., Boillee, S., Fujimori-Tonou, N., Yamashita, H., Gutmann, D.H., Takahashi, R., Misawa, H., Cleveland, D.W., 2008. Astrocytes as determinants of disease progression in inherited amyotrophic lateral sclerosis. Nat. Neurosci. 11 (3), 251–253. https://doi.org/10.1038/nn2047.